SAND82-1275

Technical Assistance for Regulatory Development:

Radionuclide Concentrations for the Basalt and Bedded Salt Repositories

R. E. Pepping

Sandia National Laboratories
Albuquerque, N. M. 87185

May 1982

Fin No. A-1165 Task 3

Table of Contents

Figures

Figures (Continued)

Tables

I. Introduction

The Nuclear Regulatory Commission (NRC) has contracted Sandia National Laboratories (SNL) to provide technical assistance for the development of regulatory standards for nuclear waste disposal. In this project simplified repository analyses of hypothetical geologic repositories have been performed. To date, analyses of bedded salt and basaltic repositories have been performed and reported [1,2]. An analysis of a reference repository in a tuff flow is underway.

These analyses use computer models to simulate the transport of radionuclides to the biosphere which results from postulated breaches of the repository. The model used for these calculations is the NWFT/DVM model developed by SNL for use by NRC [3]. NWFT/DVM calculates radionuclide specific discharge rates to the biosphere in Curies/day for the long periods expected for such releases, tens of thousands of years. The result of such calculations may be used with other computer models to estimate the environmental distribution and health effects from such releases.

In the previous analyses performed in this project, we have been working with the draft EPA Standard (40CFR191) [4].

This draft standard requires time-integration of the calculated discharge to estimate total Curie releases over a 10,000 year period. In order to understand the implications of the calculated discharge rates, additional computations have been requested of SNL by NRC. Specifically, in this document we will report the estimations of radionuclide concentrations in the groundwater transporting the radionuclides. The interest in these calculations is two fold. Since the groundwater represents a potential source of drinking water, a standard already exists which places limits on the maximum allowable radionuclide concentrations, specifically, 10CFR20 [5]. Calculations of this type may be necessary in the assessment of the expected performance of a real repository. Furthermore, at this time the potential exists for significant modification of the draft EPA Standard from its present form. Thus, in order to better understand the implications of these releases and to compare the calculated concentrations to the only existing related standard (10CFR20), these calculations are necessary.

II. Assumed Plume Description

The computational model employed, NWFT/DVM, calculates radionuclide discharges to the biosphere resulting from

postulated breaches of the geologic repository e.g., borehole penetration and fault formation. This calculation is performed by numerically solving the convective-dispersion equation in one dimension, for a radionuclide chain,

$$D_z \frac{\partial^2 C_i}{\partial z^2} - V\frac{\partial C_i}{\partial z} + R_{i-1}\lambda_{i-1}C_{i-1} - R_i\lambda_i C_i = R_i\frac{\partial C_i}{\partial t} \qquad (1)$$

where

C_i = i^{th} radionuclide chain member concentration

V = groundwater velocity

R_i = retardation factor for i^{th} radionuclide

λ_i = i^{th} radionuclide decay constant

D_z = $\alpha_L V$ = diffusion constant in the longitudinal (z) direction

α_L = longitudinal (z) dispersivity.

The calculated solution of Equation 1 is sufficient for estimation of radionuclide discharge rates at some point in the biosphere.

In order to estimate radionuclide concentrations in the flowing groundwater, Equation 1 must be extended into three dimensions,

$$D_x \frac{\partial^2 C}{\partial x^2} + D_y\frac{\partial^2 C}{\partial y^2} + D_z \frac{\partial^2 C}{\partial Z^2} - V\frac{\partial C}{\partial Z} = R_i \frac{\partial C}{\partial z} \qquad (2)$$

where, for convenience, the contaminant has been assumed to be nonradioactive.

The situation we evaluate is depicted in Figure 1. A point source (borehole) or line source (fault, fracture zone) is assumed to release radionuclides to groundwater flowing in the z-direction. After some time a stable plume develops $\left(\frac{\partial C}{\partial t} = 0\right)$ over the half-plane, $y \geq 0$. Away from the leading edge of the concentration profile in the z-direction ($z \approx Vt/R_1$), at some distance, z_o, the solution of Equation (2) is given by

$$C(x,y,z_o) = \frac{\dot{C}_o}{2\pi\sigma_x\sigma_y V} \exp\left[-\frac{1}{2}\left(\frac{x^2}{\sigma_x^2} + \frac{y^2}{\sigma_y^2}\right)\right] \qquad (3)$$

for point-sources, and

$$C(x,y,z_o) = \frac{\dot{C}_o}{2w\,V\sqrt{2\pi}\sigma_x} \exp\left[-1/2\,(\frac{x}{\sigma_x})^2\right] \times \left\{ \operatorname{erf}\left(\frac{y+w}{\sqrt{2}\,\sigma_y}\right) - \operatorname{erf}\left(\frac{y-w}{\sqrt{2}\,\sigma_y}\right) \right\} \qquad (4)$$

for line sources of width 2w on the y-direction. In Equations 3 and 4,

$$\sigma_x^2 = 2D_x z_o/V = 2\,\alpha_x z_o$$

$$\sigma_y^2 = 2D_y z_o/V = 2\,\alpha_y z_o$$

and $\dot{C}_o$ is related to the radionuclide source strength. $\dot{C}_o$ will be derived later.

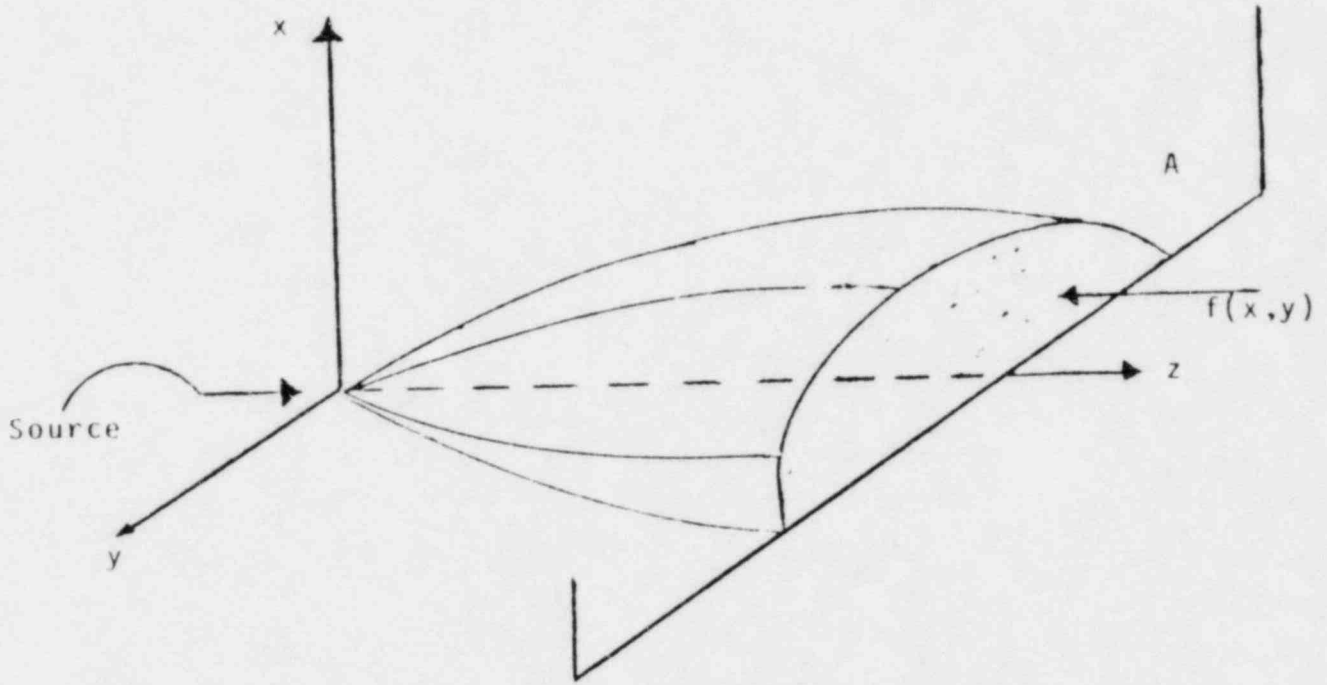

Figure 1. The Gaussian Plume

We will further assume that the medium is isotropic so that

$$D_x = D_y$$

and

$$\alpha_x = \alpha_y = \alpha_T$$

where α_T is the transverse dispersivity. Hence, we can drop the subscripts on α and note

$$\sigma^2 = 2\,\alpha_T z_o$$

Both Equations 3 and 4 are of the form,

$$C(x,y,z_o) = \frac{\dot{C}_o}{V}\, f(x,y,z_o)$$

where $f(x,y,z_o)$ describes the spatial dependence in the half-plane located at some distance from the source, z_o. The function, $f(x,y,z_o)$, is normalized to 1/2 since only the upper half-plane, depected in Figure 1, transmits radionuclides. NWFT/DVM calculates the radionuclide discharge across the half-plane depicted in Figure 1, D, which may be related to $C(x,y,z_o)$ by

$$\dot{D} = \int_A C(x,y,z_o)\,dQ = q\int C(x,y,z_o)\,dx\,dy = q\,\frac{\dot{C}_o}{V}\int f(x,y,z_o)\,dx\,dy = \frac{q\dot{C}_o}{2V}$$

Hence,

$$\dot{C}_o = \frac{2V\dot{D}}{q} \qquad (5)$$

In developing Equation 5,

Q = volumetric flow rate

q = Darcy velocity,

and q is assumed to be constant across A. Equations 3, 4 and 6 may thus be used to calculate the maximum concentrations. These occur on axis (x=y=0),

$$C_{max} = \begin{cases} \dfrac{\dot{D}}{\pi\sigma^2 q} & \text{point sources} \\ \dfrac{\dot{D}}{\sqrt{2\pi}\,\sigma w q} & \text{line sources} \end{cases} \qquad (6)$$

We note that $\dot{D}$, the NWFT/DVM result, is in fact time-dependent. The assumption of steady-state spatial distributions must then be qualified. We are actually assuming a quasi-steady-state solution in which the radionuclide source varies sufficiently slowly with time that Equations 3 and 4 adequately describe the solution to Equation 2.

The plume model used in these calculations has two associated assumptions that should be noted. Both

Equations 3 and 4 show a Gaussian behavior in the x-direction. The assumption of such behavior is valid as long as the plume's lateral extent (a few σ_x) is less than the thickness of the transporting aquifer. The plume width in the x-direction may be measured in terms of σ_x, the width parameter, where

$$\sigma_x^2 = 2\,\alpha_T z_o \qquad (7)$$

Making the assumption

$$\alpha_T = \frac{1}{10}\alpha_L$$

Equation 7 becomes,

$$\sigma_x^2 = \frac{\alpha_L z_o}{5}$$

In these calculations we will address the case, Z_o = 5,280 feet.

The values of α_L used in the calculations varied between transporting media analyzed [1, 2].

Table 1

Dispersion Properties of Transporting Units

Medium	Basalt	Bedded Salt	Bedded Salt
Transporting Unit	R	O	D
α_L range	50 feet	1-50 feet	10-100 feet
α_L distribution	fixed	Log uniform	Log Uniform
σ_x,max	230 feet	230 feet	325 feet
Thickness of Transporting Unit L_x	200 feet	300 feet	500 feet

The distributions chosen are used by a sampling technique to select specific values of α_L for each input vector. The values of $\sigma_{x,max}$ are comparable to the thickness of the transporting unit.

In cases where σ_x is much greater than the thickness of the transporting unit, denoted by L_x, the usual assumption is to replace

$$\frac{1}{\sqrt{2\pi}\,\sigma_x} \exp\left[-\frac{1}{2}\left(\frac{x}{\sigma_x}\right)^2\right]$$

in Equations 3 and 4 by L_x^{-1}. The model then describes a plume which is well mixed in the x-direction. Our situation then is neither of the cases,

$\sigma_x << L_x$ Gaussian in X

nor

$\sigma_x >> L_x$ well mixed in X

Hence, we are in the "grey" region between the two models.

With log uniform distributions, the sampling method selects a majority of small values of α_L. Hence, we expect Equations 3 and 4 to be adequate for most vectors. For a few vectors, however, the model may be in error.

The maximum concentration may be expected to be between the values given by the two models,

$$C_{max} = \frac{\dot{C}_o}{2\pi\sigma_x\sigma_y v} \qquad \text{Gaussian}$$

$$C_{max} = \frac{\dot{C}_o}{L_x\sqrt{2\pi}\sigma_y v} \qquad \text{well-mixed}$$

for point-sources, and

$$C_{max} = \frac{\dot{C}_o}{2w\sqrt{2\pi}\sigma_x v} \qquad \text{Gaussian}$$

$$C_{max} = \frac{\dot{C}_o}{2wL_x v} \qquad \text{well-mixed}$$

for line sources. We will use the Gaussian model and note that, for a few vectors, the calculated value and another value given by multiplying by a factor,

$$\frac{\sqrt{2\pi}\,\sigma_x}{L_x}$$

bound the correct value. The factor is of the order of unity.

Choice of C_{max}

We have chosen C_{max}, as given by Equation 6, to present the results of these calculations. It is useful in that it provides a quantity that can be easily manipulated in response to questions relating to regulatory development. For example, a more interesting quantity may be an average concentration across some width of the aquife, including the plume. For example, essentially all of the plume is contained in a "pipe" of diameter 6σ. The area of a plane through that pipe is

$$\frac{1}{2}\pi(3\sigma)^2$$

where the factor of 1/2 comes from considering only the half-plane shown in Figure 1. An average concentration is then given by,

$$\overline{C} = \frac{2\dot{D}}{9\pi\sigma^2 q} = \frac{2}{9} C_{max}$$

for point sources, and

$$\overline{C} = \frac{\dot{D}}{3\sigma(2w)q} = \frac{\sqrt{2\pi}}{3} C_{max}$$

for line sources.

The choice of an even larger area gives larger quantities of groundwater discharge and correspondingly lower concentrations.

Thus C_{max} is a useful quantity, from a computational point-of-view, which may be scaled to include other effects and assumptions.

Implementation

Radionuclide discharge rates were calculated with NWFT/DVM. Because of uncertainty in the data used by NWFT/DVM, Latin Hypercube Sampling (LHS) was used to select multiple sets of input (vectors) to calculate discharge rates, one discharge rate as a function of time for each radionuclide and each input vector. Latin Hypercube Sampling provides an unbiased estimate of

the cumulative distribution function of the model output (discharge rate at each time) [6].

Among the quantities sampled by LHS are hydraulic properties and dispersivities. These are used to calculate q and σ in Equation 6. To evaluate α_T ($\sigma^2 = 2\alpha_T Zo$) we make the usual assumption relating the longitudinal and transverse dispersivity,

$$\alpha_T = \frac{1}{10} \alpha_L$$

Thus, the NWFT/DVM results and the LHS chosen input vectors may be used to evaluate Equation 6 for each postulated scenario.

In the bedded salt analyses [2] multiple borehole scenarios were considered. The assumption was made in the results presented here that all released radionuclides issued from a single borehole. This assumption is conservative in that it gives a concentration, C_{max}, as given by Equation 6. For N boreholes, the concentration may be as low as C_{max}/N depending on the distance between boreholes. For the scenarios examined, N was generally less than ten.

Radionuclides Transported

We have chosen a subset of the actual radionuclide inventory for these calculations. The radionuclides transported are the actinide chains,

240 Pu → 236 U → 232 Th → 228 Ra → daughters

245 Cm → 241 Np → 241 Am → 237 Np → 233 U → 229 Th → daughters

246 Cm → 242 Pu → 238 U → 234 U → 230 Th → 226 Ra

↑

238 Pu

210 Pb → daughters

243 Am → 239 Pu → 235 U → 231 Pa → 227 Th → daughters

and seven fission and activation products

14 C, 90 Sr, 99 Tc, 126 Sn, 129 I, 135 Cs, 137 Cs

The initial inventories of these radionuclides are shown in Table 2. Short-lived daughters at the end of the actinide chains and intermediate between transported chain members are assumed to be discharged to the biosphere in equilibrium with their parents. All radionuclides are assumed to be discharged with the transverse spatial distribution of Equation 2 or 4 describing their concentration. Of interest in these calculations is the maximum concentration given by Equation 6.

Table 2

Radionuclide Inventories and 10CFR20 Limits

Radionuclide	Initial Curies	RCG or RCG_{eff} (Ci/m^3)
4n + 0		
240 Pu	4.61E7	5.E-6
236 U	3.16E4	3.E-5
232 Th	3.22E-5	2.E-6
228 Ra	8.95E-6	2.85E-8
4n + 1		
245 Cm	3.34E4	4.E-6
241 Pu	4.4E9	2.E-4
241 Am	2.E8	4.E-6
237 Np	4.04E4	3.E-6
233 U	7.96E0	3.E-5
229 Th	1.55E-2	3.76E-7
4n + 2		
246 Cm	6.64E3	4.E-8
242 Pu	1.30E5	5.E-6
238 U	3.03E4	1.33E-5
238 Pu	3.08E8	5.E-6
234 U	9.95E4	3.E-5
230 Th	1.68E1	2.E-6
226 Ra	8.09E-2	2.88E-8
210 Pb	1.78E-2	8.73E-8
4n + 3		
243 Am	1.73E6	4.E-6
239 Pu	3.19E7	5.E-6
235 U	1.6E3	2.6E-5
231 Pa	3.39	9.E-7
227 Ac	1.44	3.35E-7
Fission/Activation Products		
137 Cs		2.E-5
135 Cs		1.E-4
129 I		6.E-8
126 Sn		3.E-6
99 Tc		3.E-4
90 Sr		3.E-7
14 C		8.E-4

III. Use of 10CFR20

An existing Federal Regulation, 10CFR20 [5], regulates radionuclide concentrations in drinking water by specifying a recommended concentration guide (RCG) in Curies/m^3 H_2O for each radionuclide. For mixtures of radionuclides, such as we are considering, the standard required

$$1 \geq \sum_i \frac{C_i}{RCG_i}$$

where the sum over i denotes summation over all discharged radionuclides, C_i is the concentration of the i^{th} radionuclide, and RCG_i is given by 10CFR20 as shown in Table 4. Thus we will calculate a quantity f(c),

$$f(c) = \sum_i \frac{C_i}{RCG_i} \qquad (8)$$

In order to include the short-lived radionuclides excluded from the groundwater transport problem, we define an effective recommended concentration guide for the transported parent, $RCG_{i,eff}$,

$$\frac{1}{RCG_{i,eff}} = \sum_j \frac{f_j}{RCG_j} \qquad (9)$$

The sum in Equation 9 includes all daughters of radionuclide i not included in the groundwater transport problem. The f_j relate the activity of the j^{th} daughter to that of the transported parent, i. They deviate from unity due to branching. The $RCG_{i,eff}$ are shown in Table 2. Figures 2 through 5 show the four actinide decay chains that were transported and include the short-lived daughters which must be included in Equation 9. The f_j may be calculated analytically but were inferred empirically from an ORIGEN calculation [7].

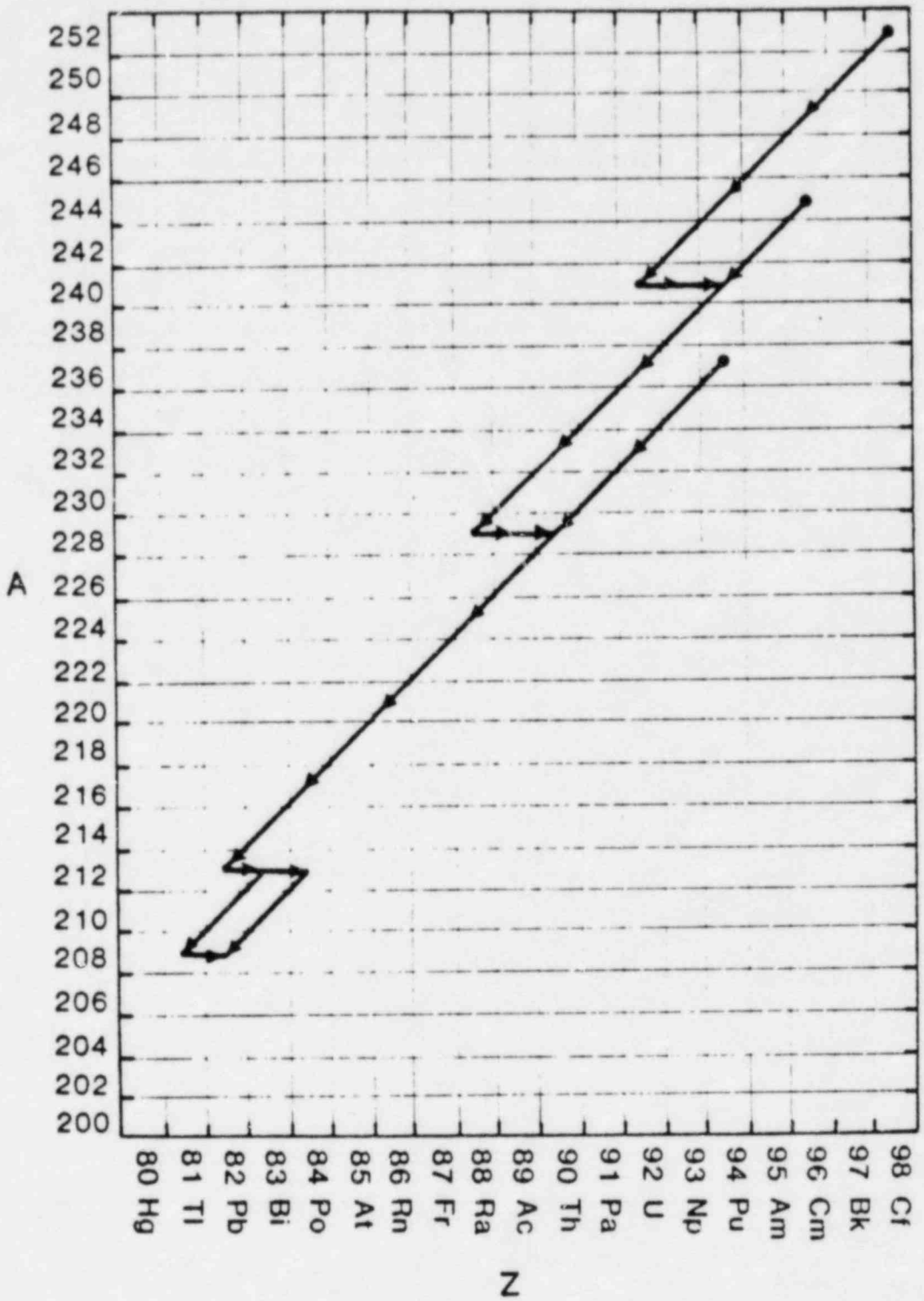

Figure 2. The 4n + 0 Series

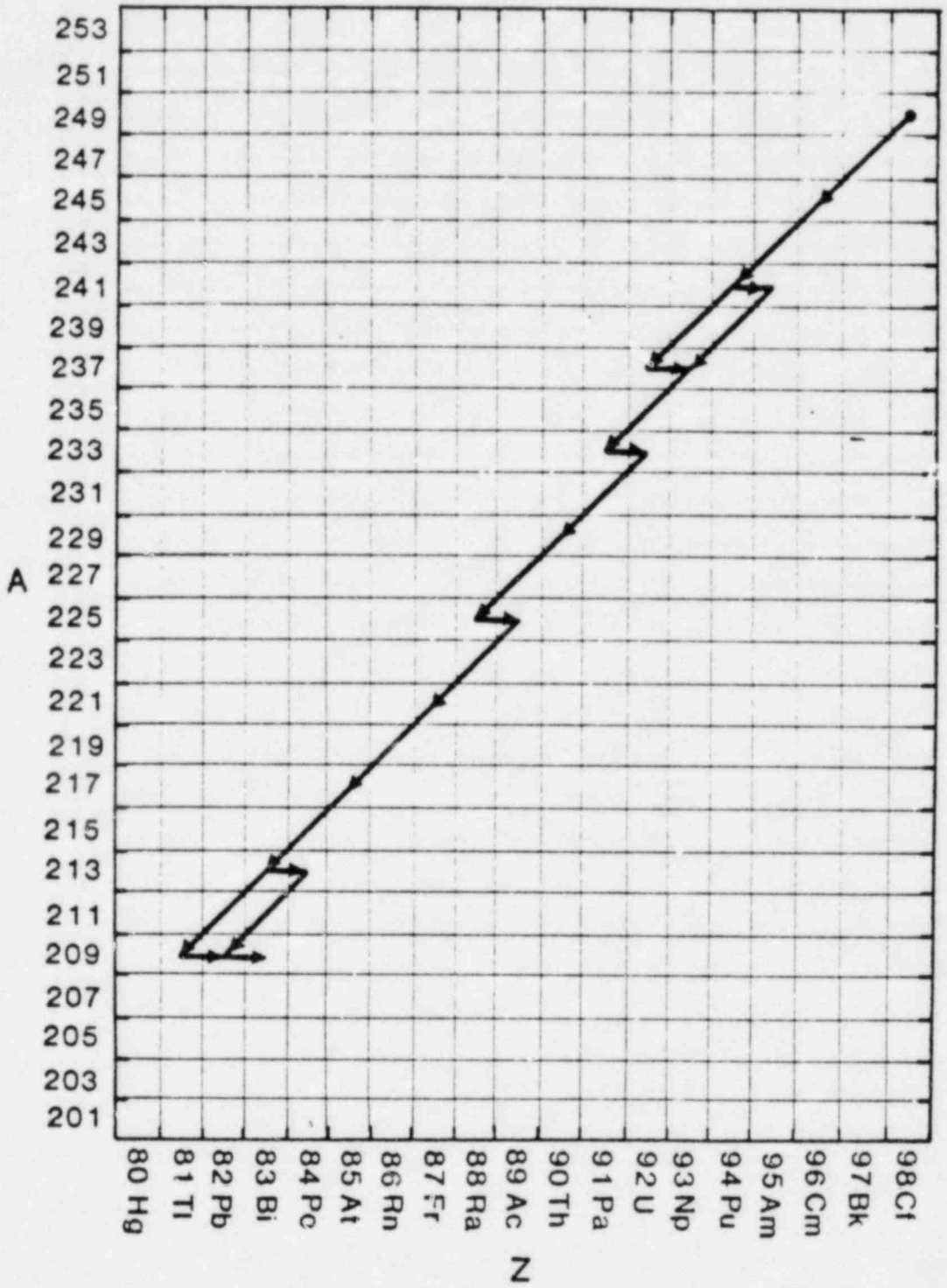

Figure 3. The 4n + 1 Series

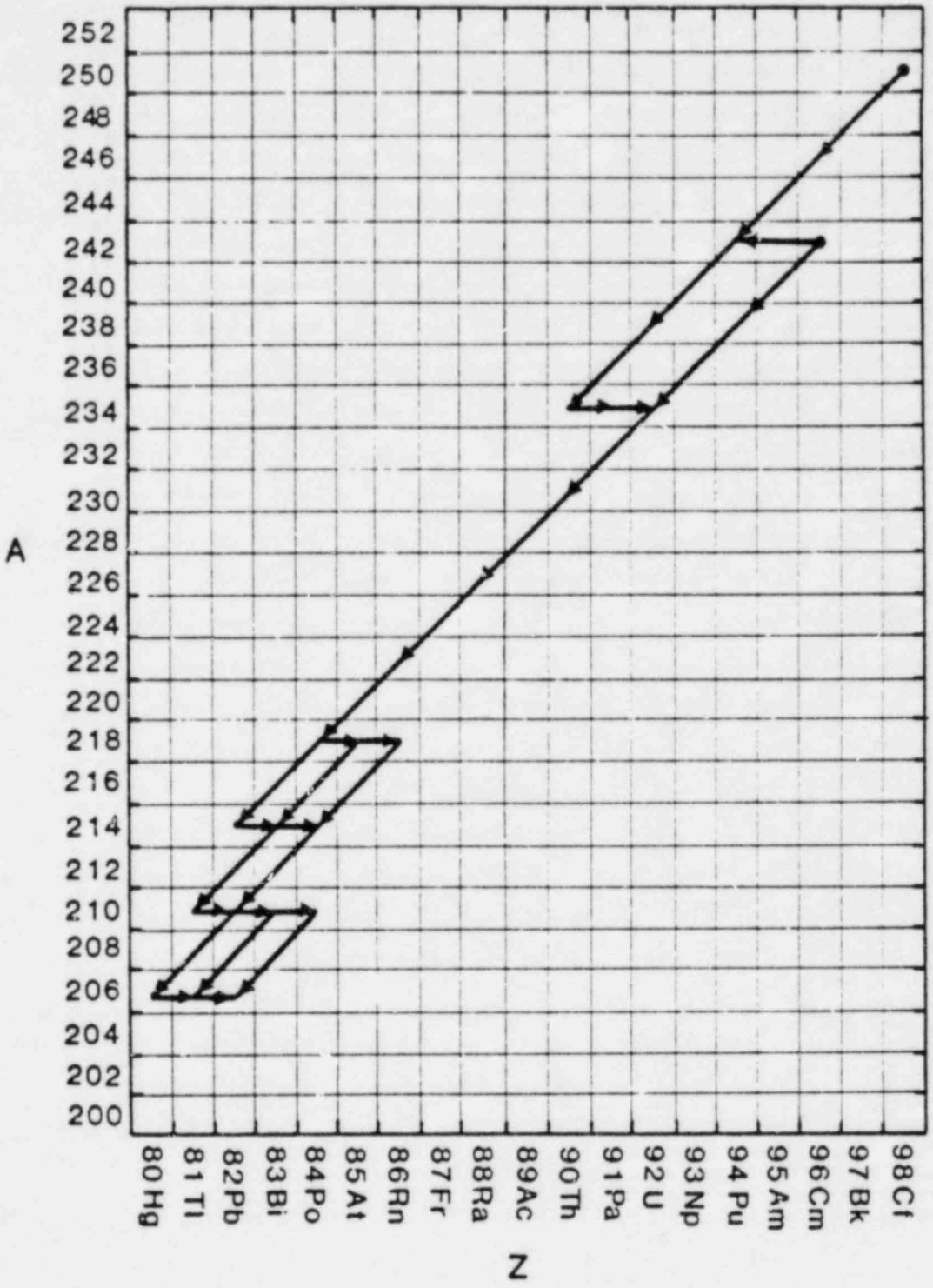

Figure 4. The 4n + 2 Series

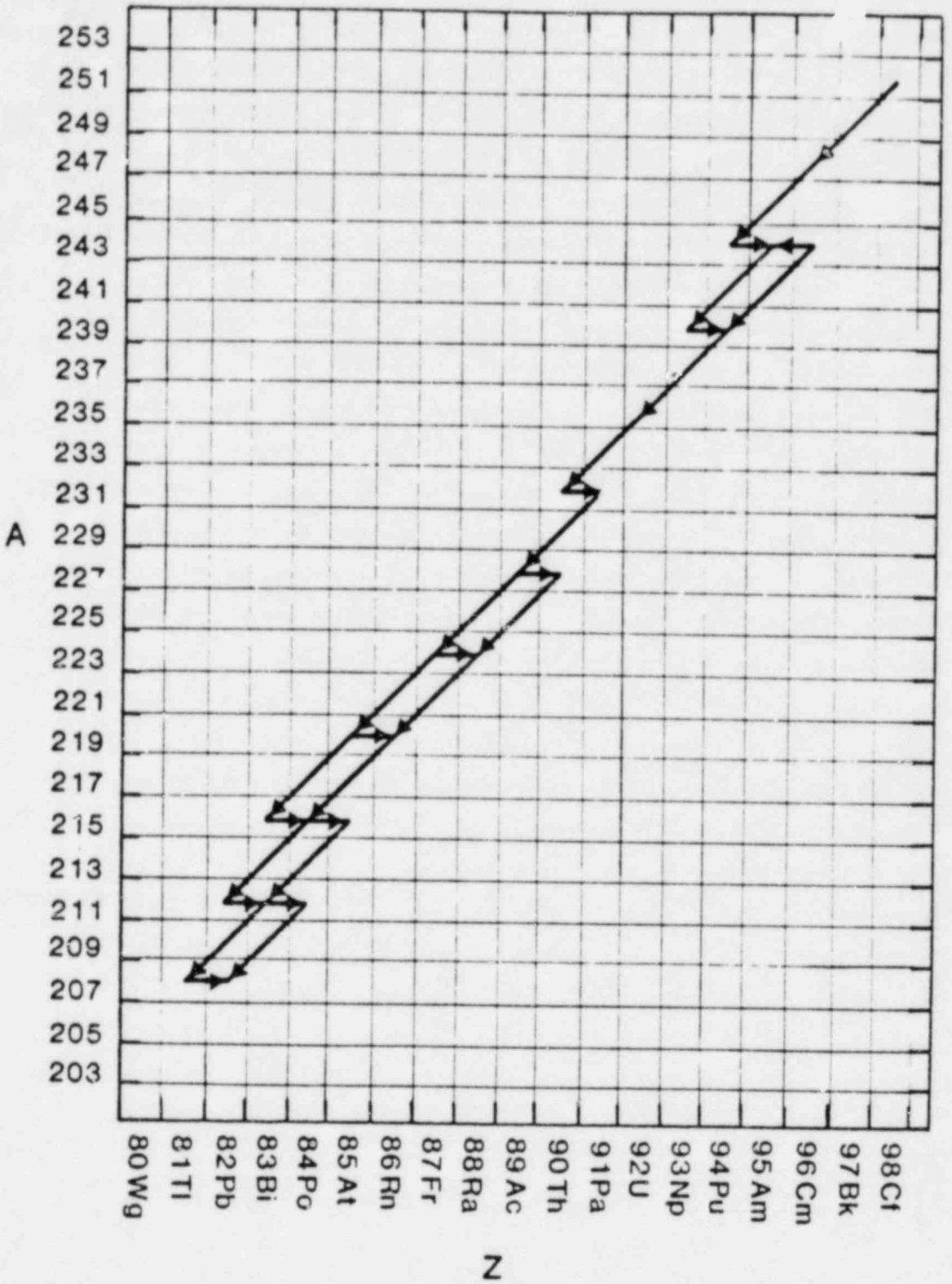

Figure 5. The 4n + 3 Series

IV. Computation Results

The methods developed in the preceding discussion were applied to results from two analyses previously reported [1, 2]. The first analysis reported [1] examined a hypothetical geologic repository in basalt. The second [2] examined a hypothetical bedded salt repository.

In the basalt analysis, three scenarios* were examined. In addition, one scenario was evaluated using two models for the radionuclide source term for the groundwater transport model. The scenarios analyzed were

Scenario	Description	Source
1	undisturbed case	leach limited
2	fractures in dense basalt	leach limited
3	borehole penetration	leach limited
4	borehole penetration	mixing cell

Scenarios 1 and 2 involved vertical flow and radionuclide migration to an overlying aquifer. The cross-sectional area of the column of flowing water was

*A scenario is defined as a unique set of events or processes which lead to radionuclide release. Each scenario has an associated flow geometry and transport variables, as determined by LHS, which are assumed to remain constant throughout a 50,000 year transport calculation.

large, comparable to the area of the subsurface facility, and treated as a line source of radionuclides into the overlying aquifer. Scenarios 3 and 4 were treated by assuming point-sources of radionuclide discharge into the overlying aquifer.

All input vectors for Scenarios 1 and 2 were evaluated with a leach-limited source assumption as selected by a source-term selection algorithm in NWFT/DVM. For Scenario 4, this algorithm selected the mixing cell model. For comparison, a leach limited source was imposed and the scenario was evaluated as Scenario 3.

In the analysis of the bedded salt repository, four groundwater transport scenarios were examined [2]. Each scenario involved borehole penetrations and failed shaft seals making a U-tube flow path. Each scenario was evaluated with three different source models. These models were described previously [2] and are summarized here. All scenarios were assumed to represent point sources of radionuclides discharging into the overlying aquifer.

Source #1: the entire radionuclide inventory is assumed to be available for transport. The radionuclides are released at leach-limited rates sampled from the range, 10^{-5}-10^{-7}/year.

Source #2: a restricted fraction of the radionuclide inventory is assumed to be available for transport. The fraction is given by assigning one roomful of waste to each borehole in the input vector determined by LHS. There are 106 rooms in the reference design. Such an assumption may be valid if groundwater flow was confined to the immediate vicinity around the borehole. The leach rate range sampled is the same as for Source #1.

Source #3: Source #2 is assumed but in addition, the backfilled rooms are treated as a mixing cell. Radionuclide release then occurs at a rate sensitive to the radionuclide concentration in the mixing cell. (This is the standard SNL source assumption.) For this source, leach rates were sampled from the range, 10^{-3}-10^{-7} year.

Data used in the groundwater transport calculation was reported previously [1,2]. Data selection (input vectors) was made by the LHS method.

The results of these calculations are presented in figures that follow. Each input vector of the NWFT/DVM calculation produces discharge rates which are used to evaluate Equations 6 and 8 at each time. There are simply too many input vectors to present the results for each of them. We have chosen four forms to present results:

1) At each time, the values of Equation 8 are examined for the whole set of vectors to determine a mean value.

2) At each time, the values of Equation 8 are examined for the whole set of vectors to determine a maximum value.

3) For each vector, the maximum value of Equation 8 (over time) is recorded. Since each input vector chosen by the LHS method is equally probable, the result can be used to estimate the distribution of maximum values of Equation 8 that may occur any time during the 50,000 year interval. The probability that the scenario will occur is not included in this construction.

4) For each vector calculated, the dominant contributors to Equation 8 were recorded. This result was tabulated for each vector and scenario in summary tables. The tables indicate the number of vectors that the given radionuclide had a first or second ranking. An entry in the tables does not necessarily mean that the vector produced a large value of Equation 8.

Basalt Scenarios: Mean Values

In Figures 6a through 9a, mean values of Equation 8 versus time are shown. Scenarios 1 and 2 are noticeably lower than Scenario 3 for the leach limited cases. All of the basalt scenarios are characterized by relatively rapid transport through the overlying aquifer. Also, for leach limited sources, the rate of radionuclide release is independent of the quantity of water flowing through the backfilled regions. Thus it appears that the differences between Scenarios 2 and 3 can be explained in terms of two causes: (1) the earlier breakthrough time associated with the borehole, and (2) the larger dilution volumes associated with the line source.

The mixing cell source term of Scenario 4 greatly reduces the expected concentrations and shows the importance of the source term assumption. The concentrations are

actually lower than those of the undisturbed case with a leach limit, Scenario 1. Ordinarily, the undisturbed case gives a small consequence compared to that of the disturbed case. For Scenarios 1 and 4 this does not appear to be the case. Scenario 4 is presented only as a demonstration of the importance of the source. Some combination of the two scenarios may be a more appropriate choice for this analysis.

Maximum Values

Figures 6b through 9b show the maximum value of Equation 8 for the four scenarios. Most of the discussion of the mean values is appropriate here also.

Maximum Value Distributions

The maximum values of Equation 8 for each vector at any time are plotted as a Complimentary Cumulative Distribution Function (CCDF) giving the fraction of input vectors producing values of Equation 8 exceeding a value denoted as CSUM. The CCDFs are shown in Figures 10 through 13. Noting the requirements of 10CFR20, the value of unity in these figures is a reference. All 100 input vectors produced values of CSUM less than unity for Scenarios 1 and 4. Scenario 2 gives approximately 3

percent of the vectors exceeding unity. Scenario 3 gives about 30 percent of the vectors exceeding unity.

Important Radionuclides

The individual radionuclides' contributions to Equation 6 were examined at each time and for each vector. The dominant two radionuclides were recorded at each time to produce a list of radionuclides that were important at some time during the calculation of that vector. These results are shown in Table 3. An entry in this table indicates that the radionuclide had a first or second ranking for the specified number of vectors.

Table 3

Important Radionuclides for Basalt Scenarios
(100 vectors, maximum)

	Scenario			
Radionuclide	1	2	3	4
240Pu			33	12
241Am			1	1
237Np			35	19
233U			5	
229Th			6	
238U			1	
234U			8	10
226Ra			46	43
210Pb			33	38
243Am			3	11
239Pu			31	11
227Ac			1	
99Tc	8	63	20	27
126Sn		1	1	
129I	58	99	100	96
14C	99	99	100	100

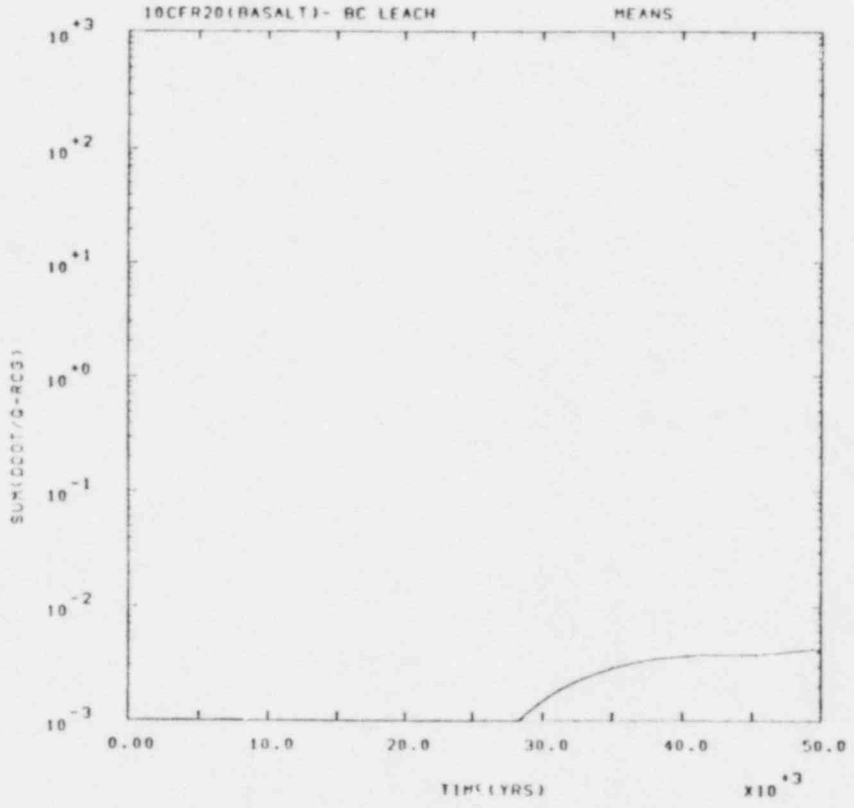

(a)

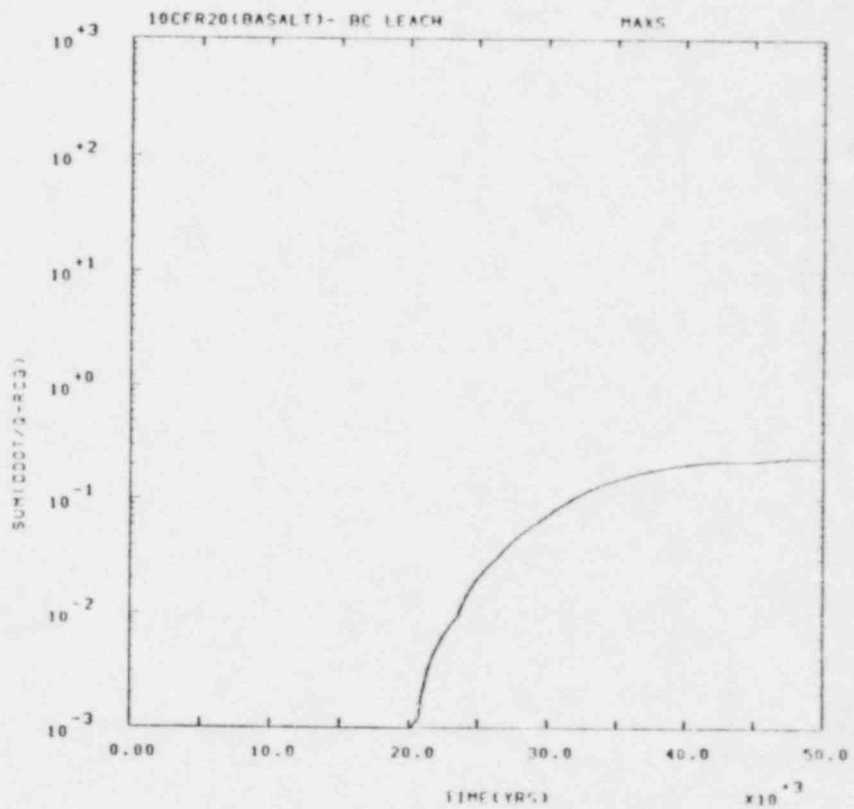

(b)

Figure 6. Basalt Scenario 1: the base case, mean and maximum versus time

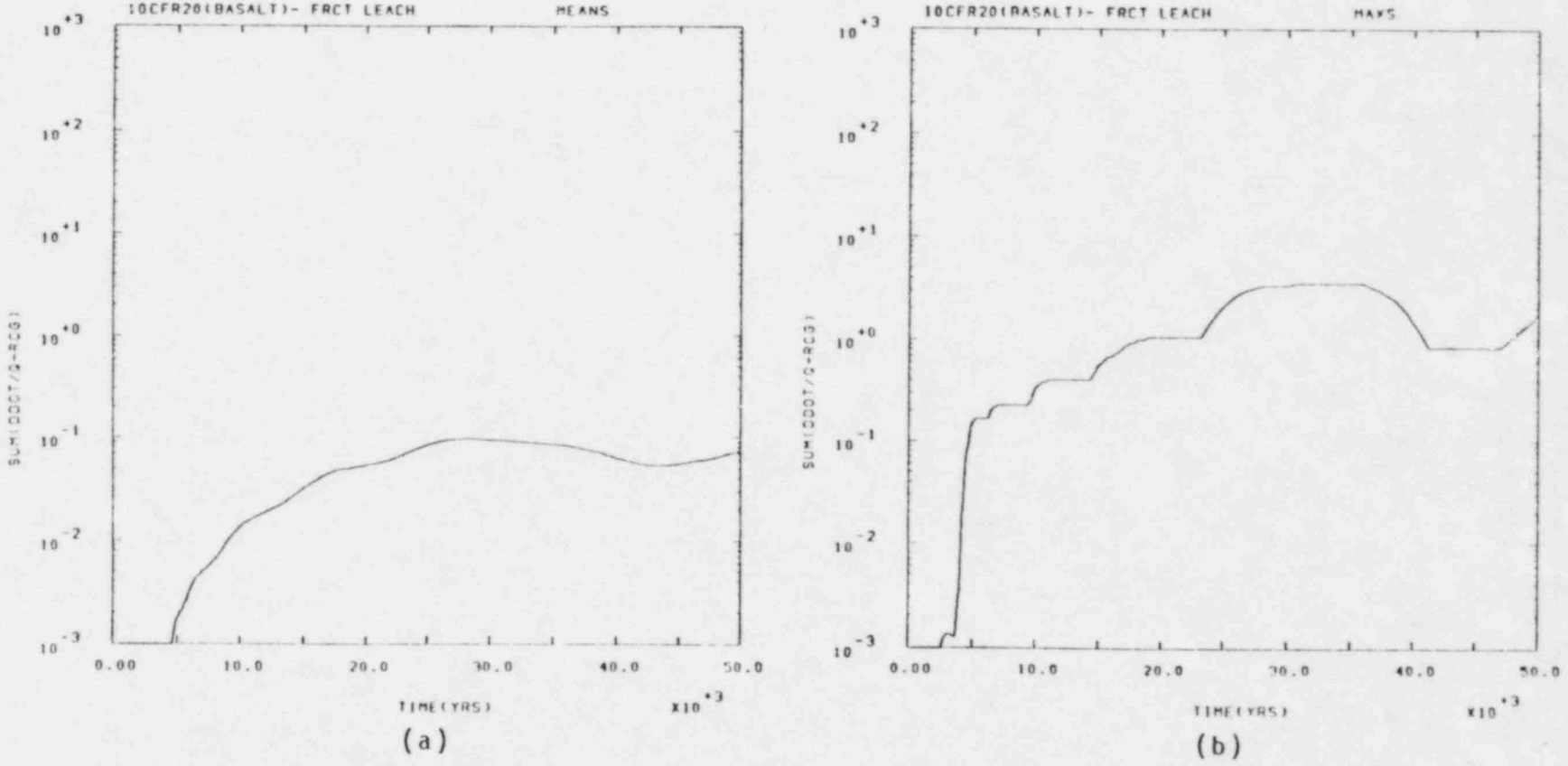

Figure 7. Basalt Scenario 2: fractures in dense basalt, mean and maximum versus time

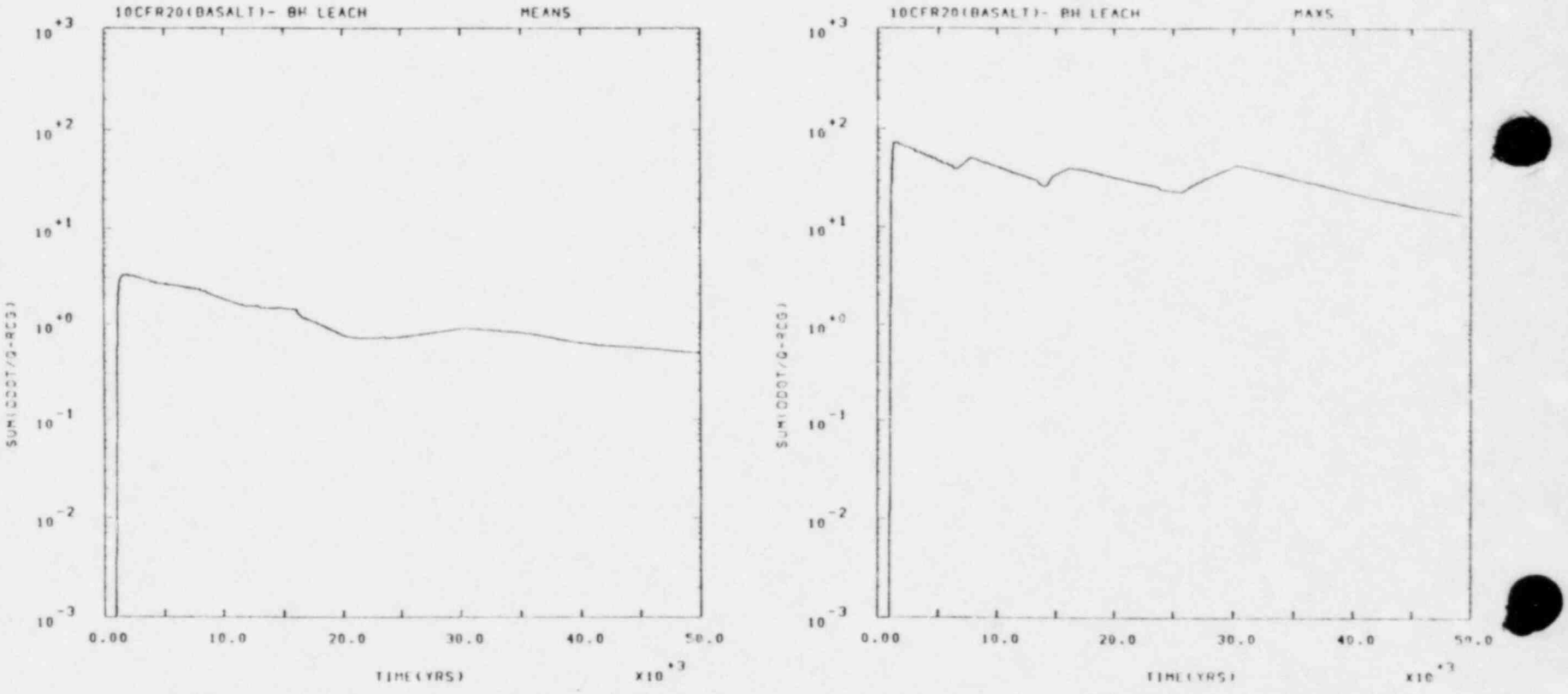

Figure 8. Basalt Scenario 3: the borehole, leach limited, mean and maximum versus time

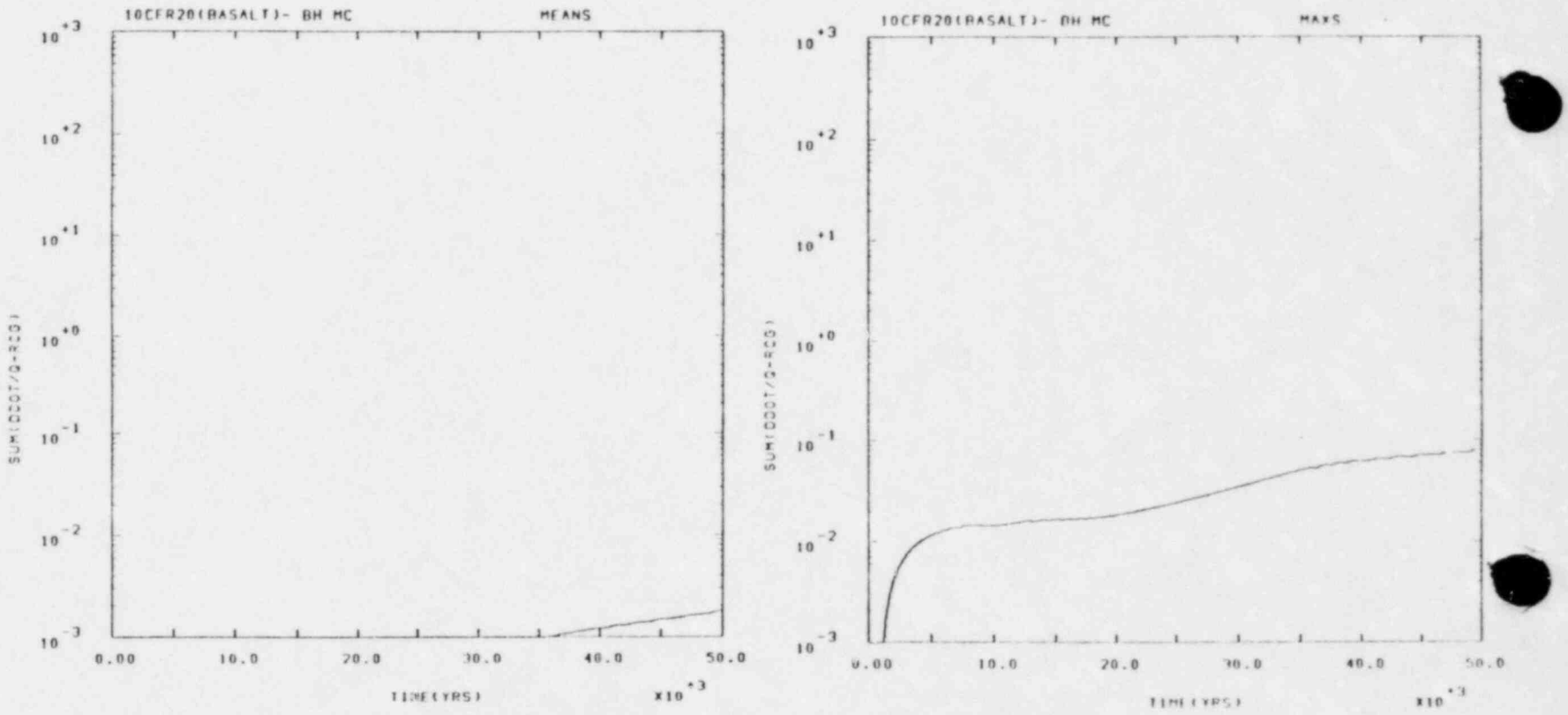

Figure 9. Basalt Scenario 3: the borehole, mixing cell, mean and maximum versus time

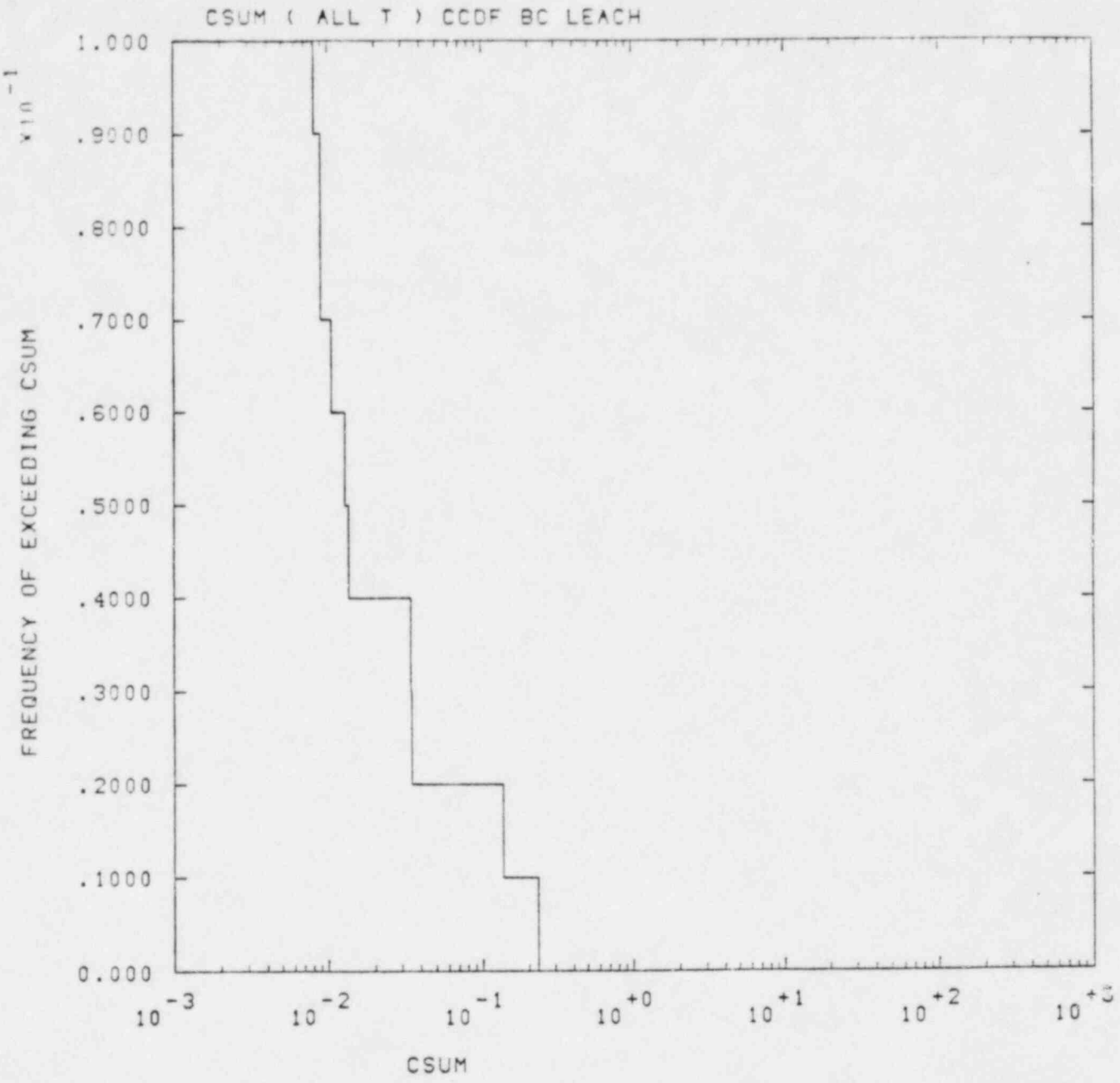

Figure 10. CCDF for Basalt Scenario 1, maximum concentrations

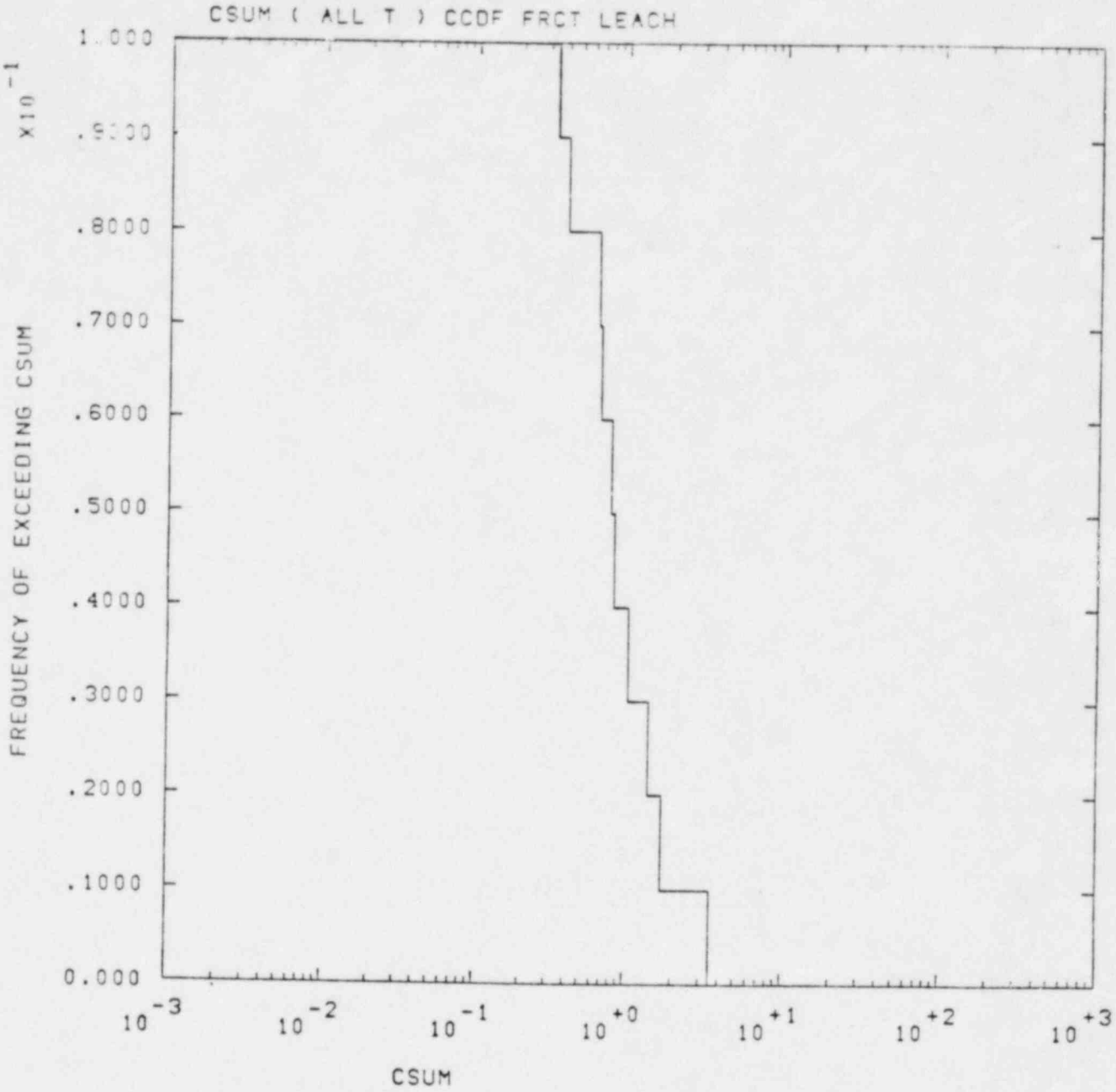

Figure 11. CCDF for Basalt Scenario 2, maximum concentrations

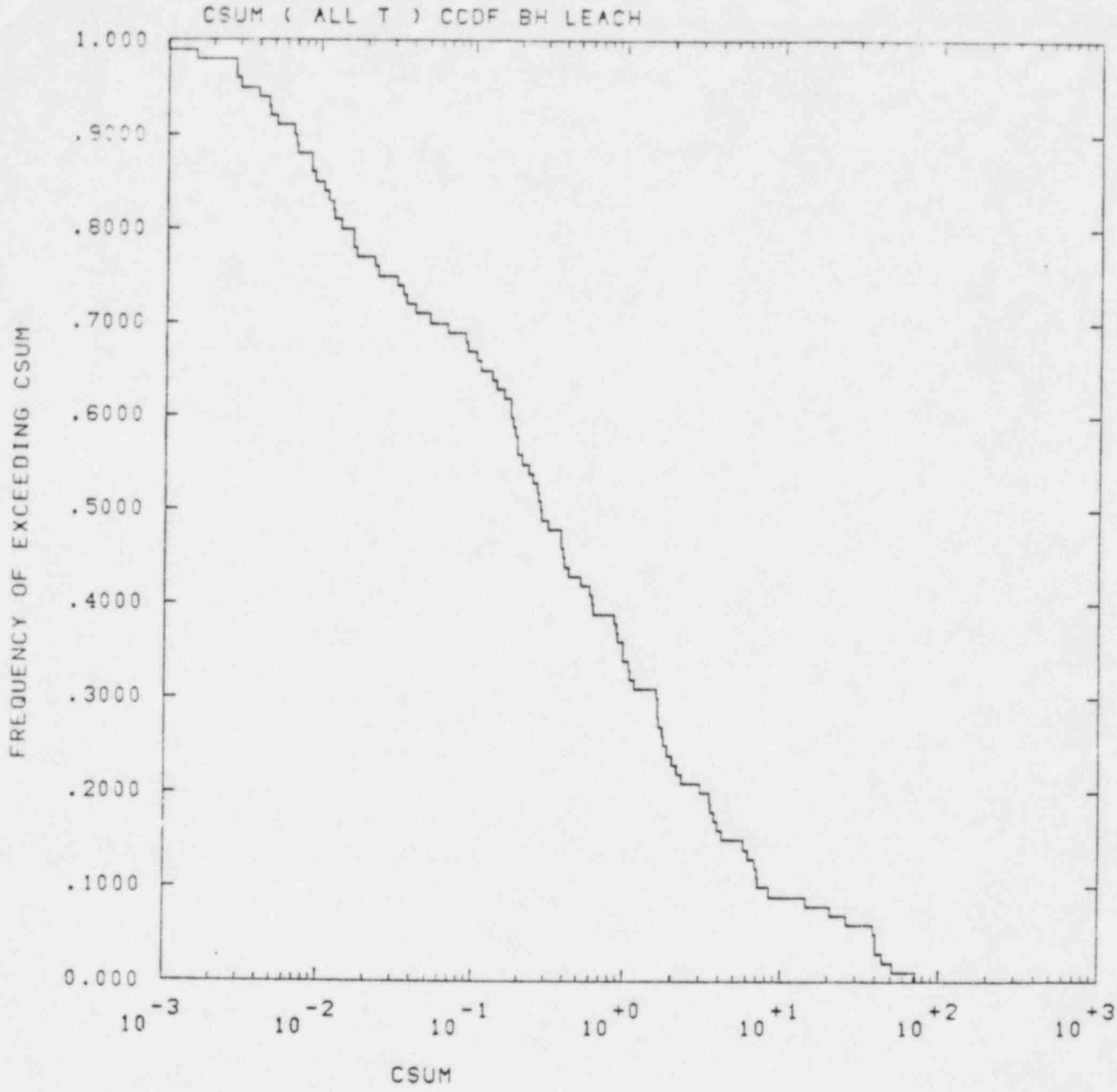

Figure 12. CCDF for Basalt Scenario 3 (Leach Limited), maximum concentrations

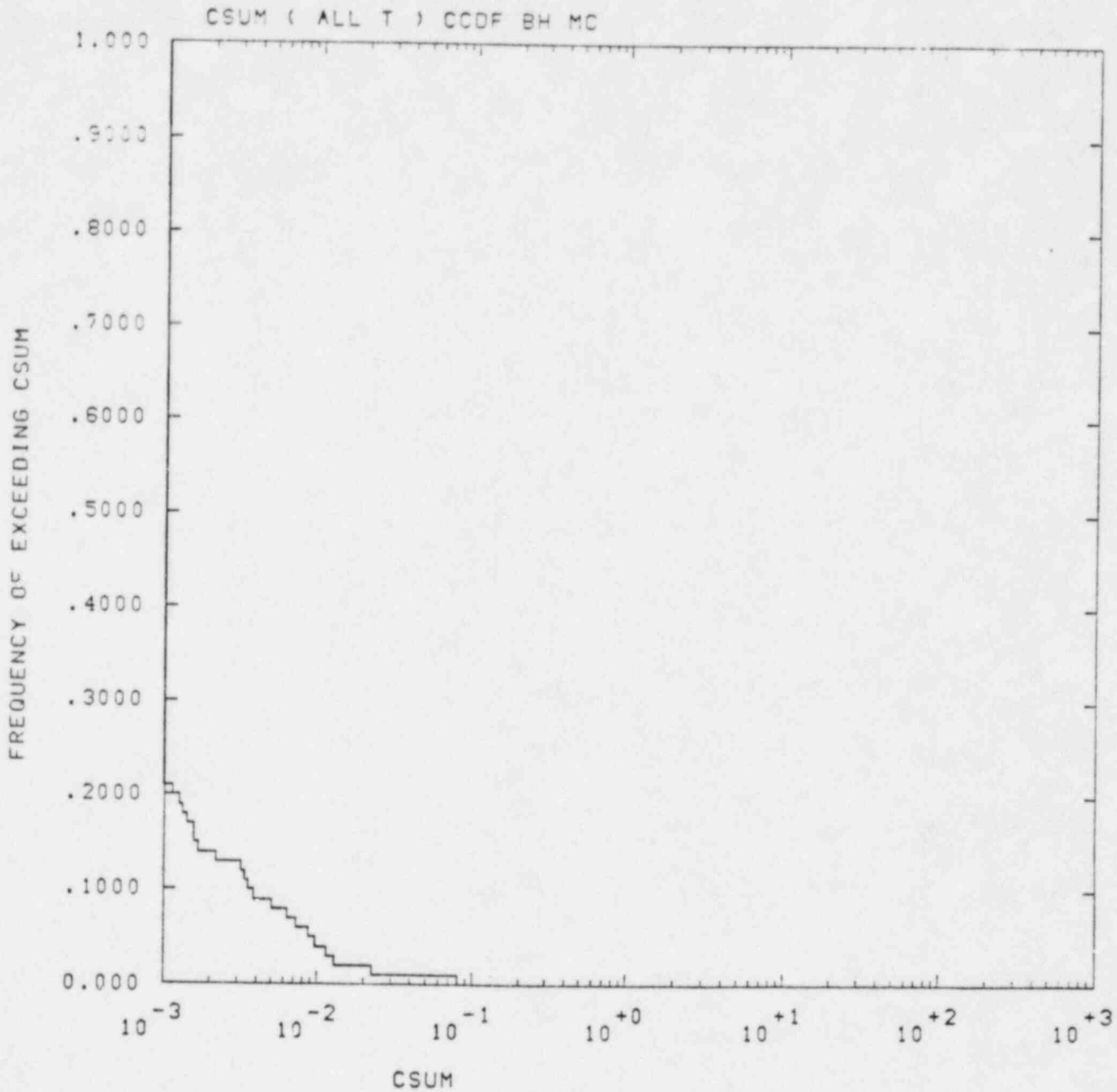

Figure 13. CCDF for Basalt Scenario 3 (Mixing Cell), maximum concentrations

Bedded Salt Scenarios

Before discussing the numerical results of the analyses of the bedded salt scenarios, we will discuss some of the general behavior expected of Equation 6 since the bedded salt scenarios seem to demonstrate them so clearly. The scenarios analyzed involve different combinations of failed shafts and boreholes with radionuclide transport to the accessible environment occurring through one of two possible overlying aquifers. In all scenarios, failed boreholes release radionuclides to the overlying aquifer and are modeled as point sources.

In the bedded salt scenarios, replicated sampling was used to estimate the magnitude of sampling error. In doing so, independent samples of input data were evaluated with the models described. The results of evaluations with each set are presented simultaneously. By doing this, the variation in calculated results due simply to sampling error are demonstrated.

Three sources were assumed in these analyses, two of which are leach limited. The third source assumed models the backfilled region as a mixing cell. Radionuclides are assumed to be released from the waste packages at a specified rate (the leach rate) into the mixing cell where they mix with groundwater. Release rate for the groundwater transport calculation are governed by their

concentrations in the mixing cell and their residence time in the cell. The residence time in the mixing cell is in turn governed by the rate of groundwater flow through the cell and its flow velocity. This source model has been described in appendices to References 1 and 2.

The first two sources assume radionuclide release rates from the backfilled regions to occur at leach limited rates. Only the fraction of wastes accessed by the flowing groundwater is assumed to vary, as discussed previously. For leach limited sources, the characteristics of groundwater flow through the backfilled regions do not influence the release rate. All other things being the same, the release rate is then simply related to the fraction of waste accessed. We take care of the "all other things being equal" condition by using the same imput vectors for all calculations, the same conductivities, sorption constants, porosities, etc., for each analysis.

For the leach limited sources, Equation 6 may be used to estimate the behavior expected in the calculated results. The relationships derived will be crude, based on mean values, but will be useful in making order-of-magnitude estimates of the behavior expected as the source model assumption or scenario are varied.

From Equation 6 we expect the variables affecting q and to affect the calculated results. The Darcy velocity, q, is given by,

$$q = Ki$$

where K is the hydrauiic conductivity, a sampled quantity, and i is the hydraulic gradient in the aquifer assumed to be constant at .007. For Scenarios 3 and 4, the value of K was chosen to be 1/10 of the value for the same input vector in Scenarios 1 and 2. The dispersivities, which affect σ, are chosen according to the LHS method from the distributions shown in Table 1. A single loguniform distribution was sampled to determine a value of the dispersivity from the assumed range in Table 1. Thus, a sampled value of α = 1.0 feet in Scenarios 1 and 2 was transformed to give a value of α = 10 feet in Scenarios 3 and 4.

The distributions shown in Table 1 and the value of K assumed may be used to estimate the expected relative behavior. Letting a subscript, n, denote the scenario and m denote the source, the value of Equation 6 for a similar scenario with a leach limited source may be estimated relative to a reference scenario

$$C_{max,n,m} = \left(\frac{q_{ref}}{q_m}\right)\left(\frac{\sigma^2_{ref}}{\sigma^2_n}\right)\frac{(\text{access fraction})_{n,m}}{(\text{access fraction})_{ref}} C_{max,ref}$$

$$= \left(\frac{K_{ref}}{K_n}\right)\left(\frac{\alpha_{ref}}{\alpha_n}\right) \frac{(\text{access fraction})_{n,m}}{(\text{access fraction})_{ref}} \cdot C_{max,ref}$$

For example, for Source #1 we assumed all access fractions to be unity. Taking Scenario 1 as the reference, Scenario 2 would be expected to give a very similar result since both scenarios assume transport to occur through the same unit (same K and α). The Scenario 3 result could be estimated from Scenario 1 by estimating the α-ratio by the geometric means of the Table 1 extremes,

$$\left(\frac{K_1}{K_3}\right)\left(\frac{\alpha_1}{\alpha_3}\right) = 10 \left(\frac{7.07}{31.6}\right) \approx 2.2$$

For the scenarios analyzed, this term is always unity or 2.2.

The access fraction for Source 2 (and for Source 3) was determined from an estimated number of boreholes leading to the scenario [2]. The accessed fraction was proportional to this number. Thus, the relative access fraction (relative to unity) can be estimated from the number of boreholes expected. Each borehole was assumed to access one of 106 rooms full of waste.

	Expected Access Fraction			
Scenario	1	2	3	4
Source				
1	1.0	1.0	1.0	1.0
2 or 3	.015	.024	.030	.034

Numerical Results

Figures 14 through 21 show the mean and maximum values of Equation 8 versus time. The predicted behavior above is followed reasonably well for the mean values plotted for Sources #1 and #2. The behavior of the maximums is somewhat less satisfactorily in agreement with prediction. Sampling error is acceptably small for the means and larger for the maximums, as may be expected. CCDF's have also been constructed for these scenarios and are shown in Figures 22 through 25. Sampling error is again small. The CCDF's are useful in assessing the likelihood of compliance with 10CFR20. The mean and maximum values versus time of Equation 8 are shown in Figures 26 through 29 for the four scenarios with Source #3. In examining results of analyses with the mixing cell source model (Source #3), the results of Source #2 are most relevant. Both Sources #2 and #3 are assumed to access the same fraction of waste for each input vector. The release rate for the mixing cell model asymptotically approaches that of the leach limited release rate with a time-dependence given by the mean residence time of the radionuclides in the mixing cell [1,2]. Thus, the value of Equation 8 for a given input vector is lower for Source #3 than for Source #2 even though the leach rate for Source #3 was sampled from a

higher range than for Source #2 as discussed previously. CCDF's for the four scenarios are shown in Figures 30 through 33. From these results it appears that the mixing cell assumption, if justifiable, could compensate for a less stable waste form.

Important radionuclides are shown in Table 4. For Sources #1 and #2, the rankings are identical since the source models are simply related. For Source #3 the release rate for several vectors is so low that no discharge occurs.

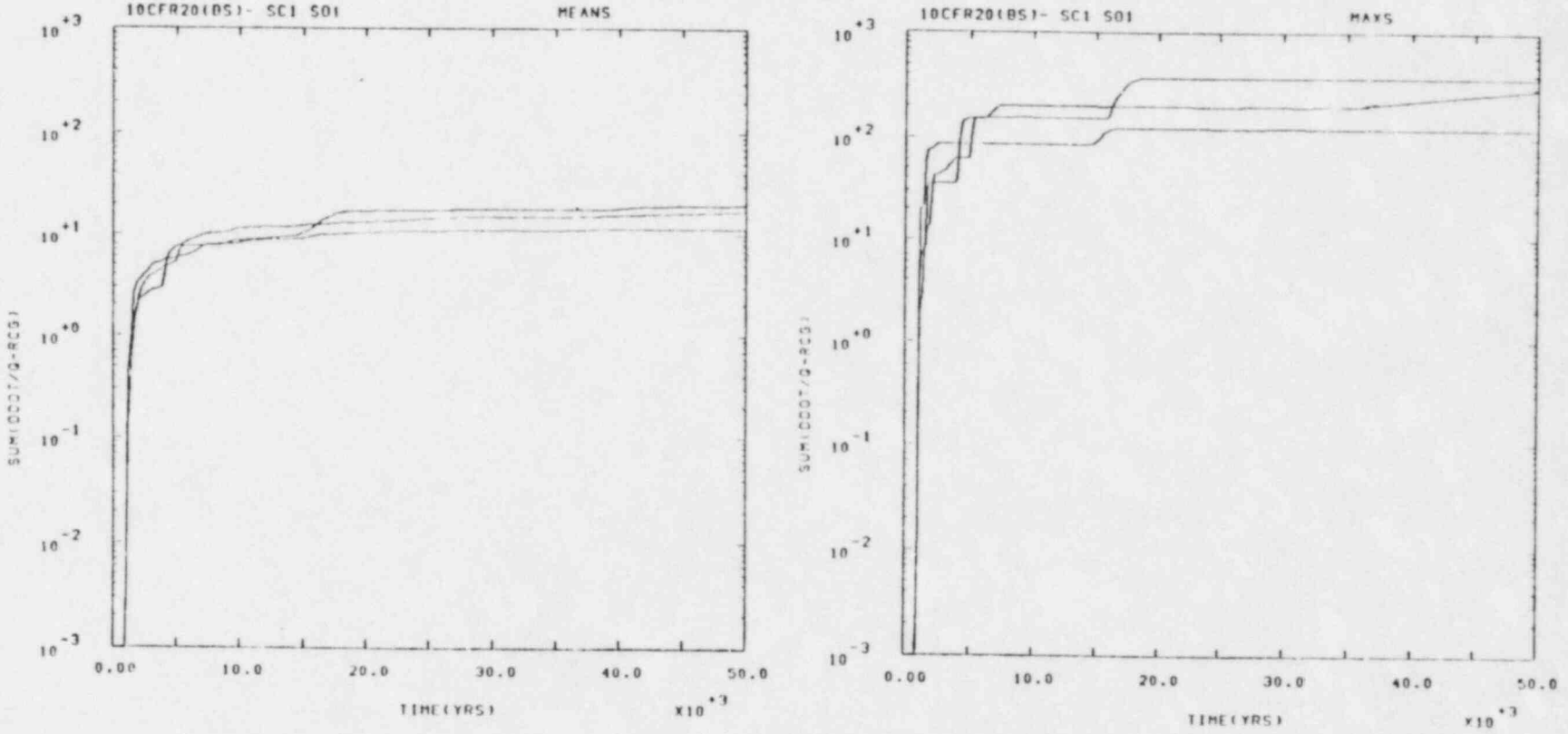

(a) (b)

Figure 14. Bedded Salt Scenario 1, Source 1, mean and maximum versus time

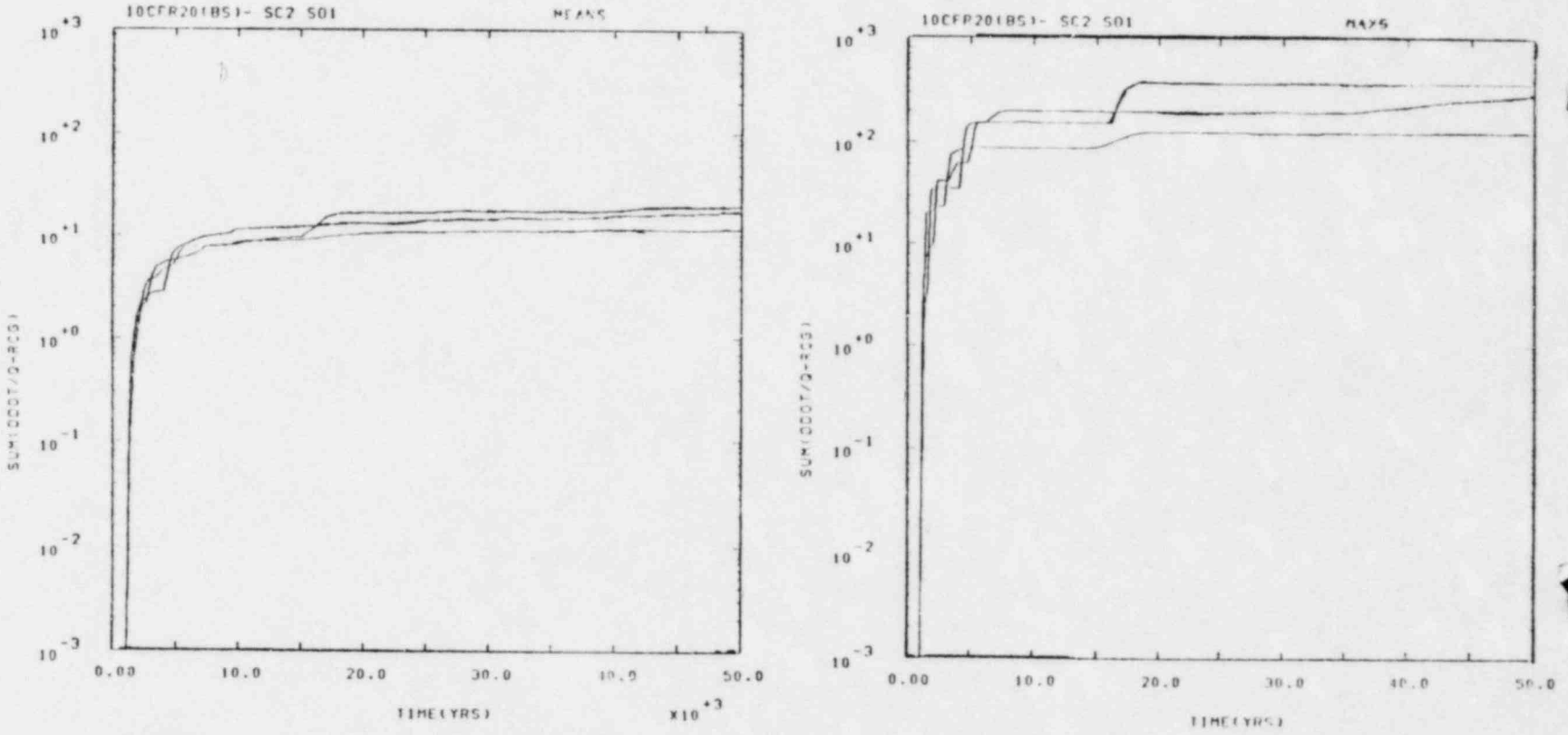

(a) (b)

Figure 15. Bedded Salt Scenario 2, Source 1, mean and maxiumum versus time

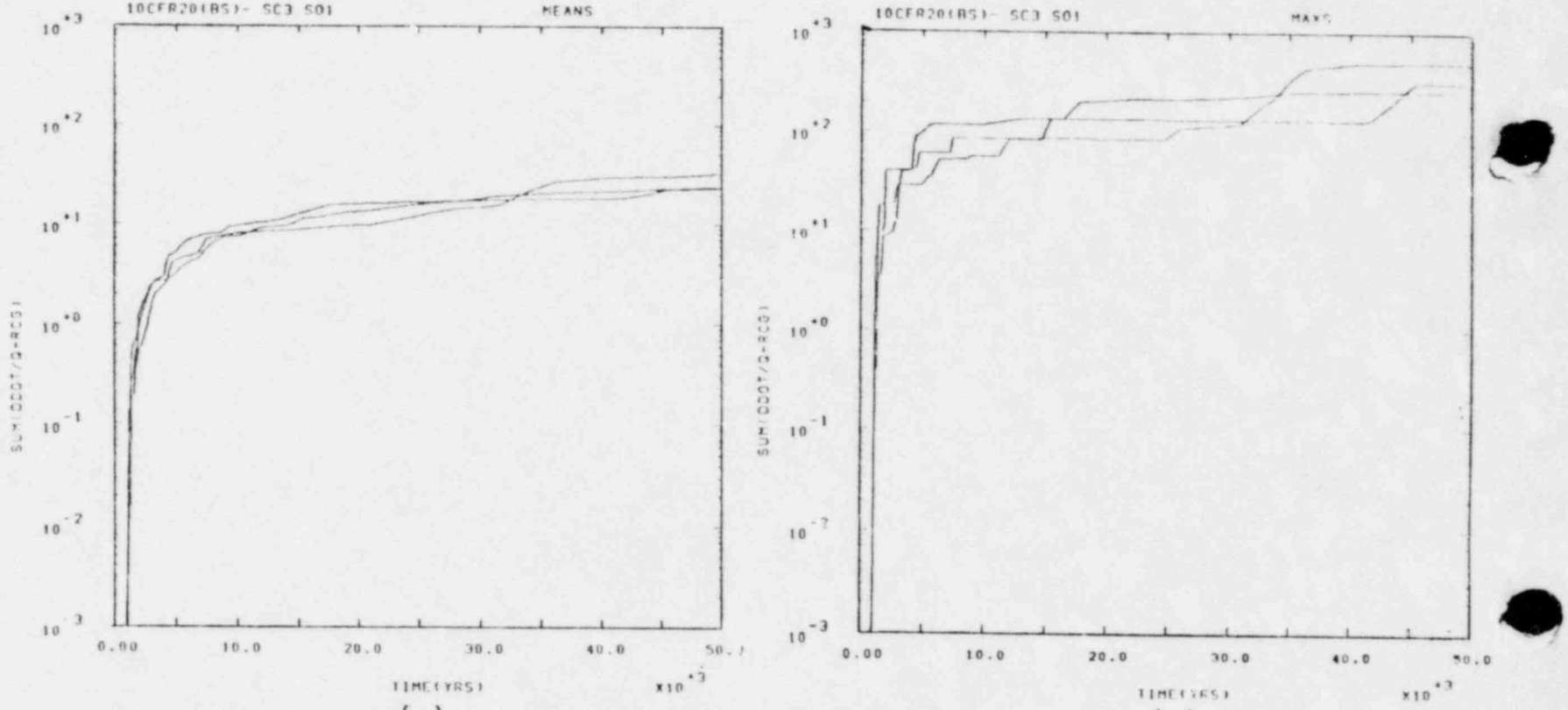

Figure 16. Bedded Salt Scenario 3, Source 1, mean and maximum versus time

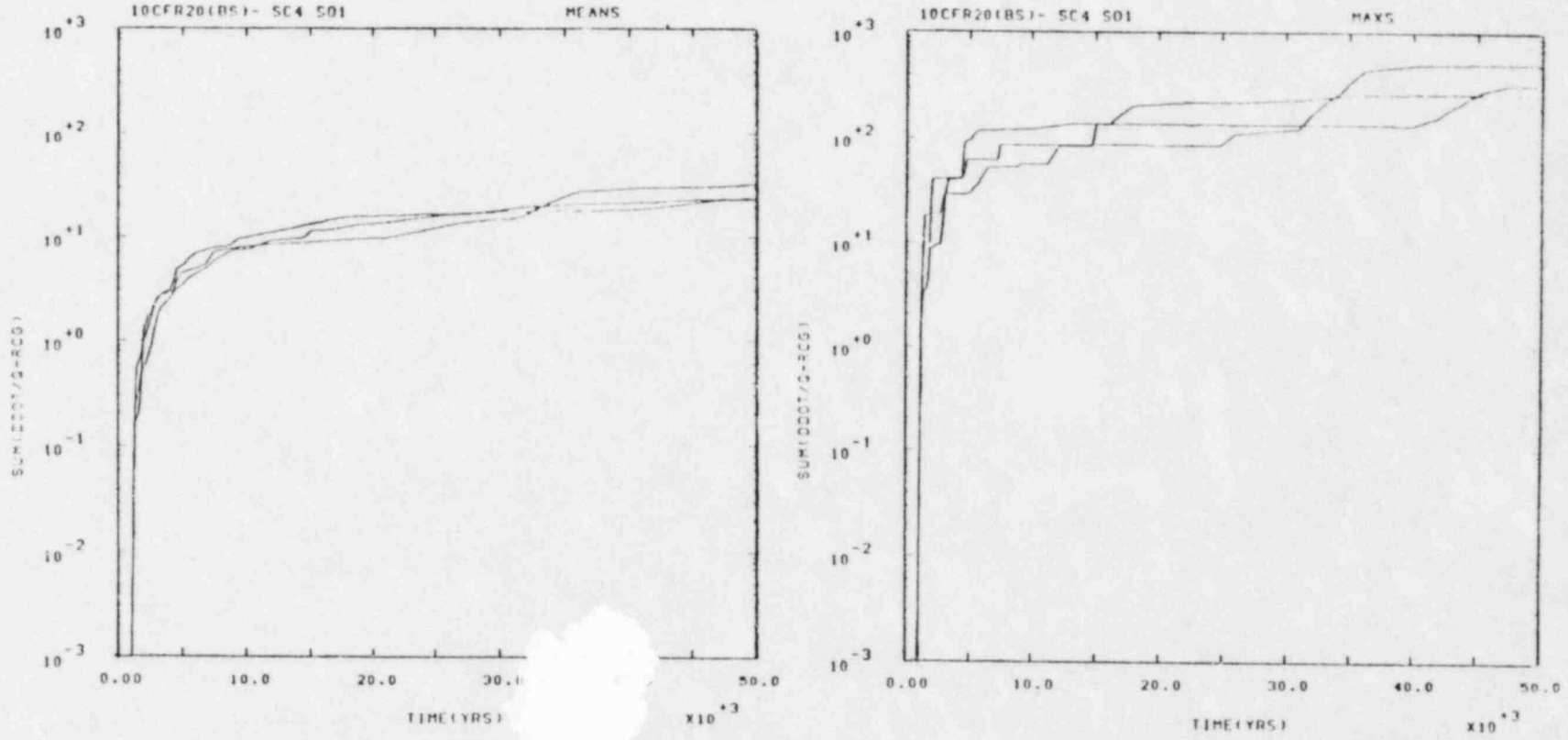

Figure 17. Bedded Salt Scenario 4, Source 1, mean and maximum versus time

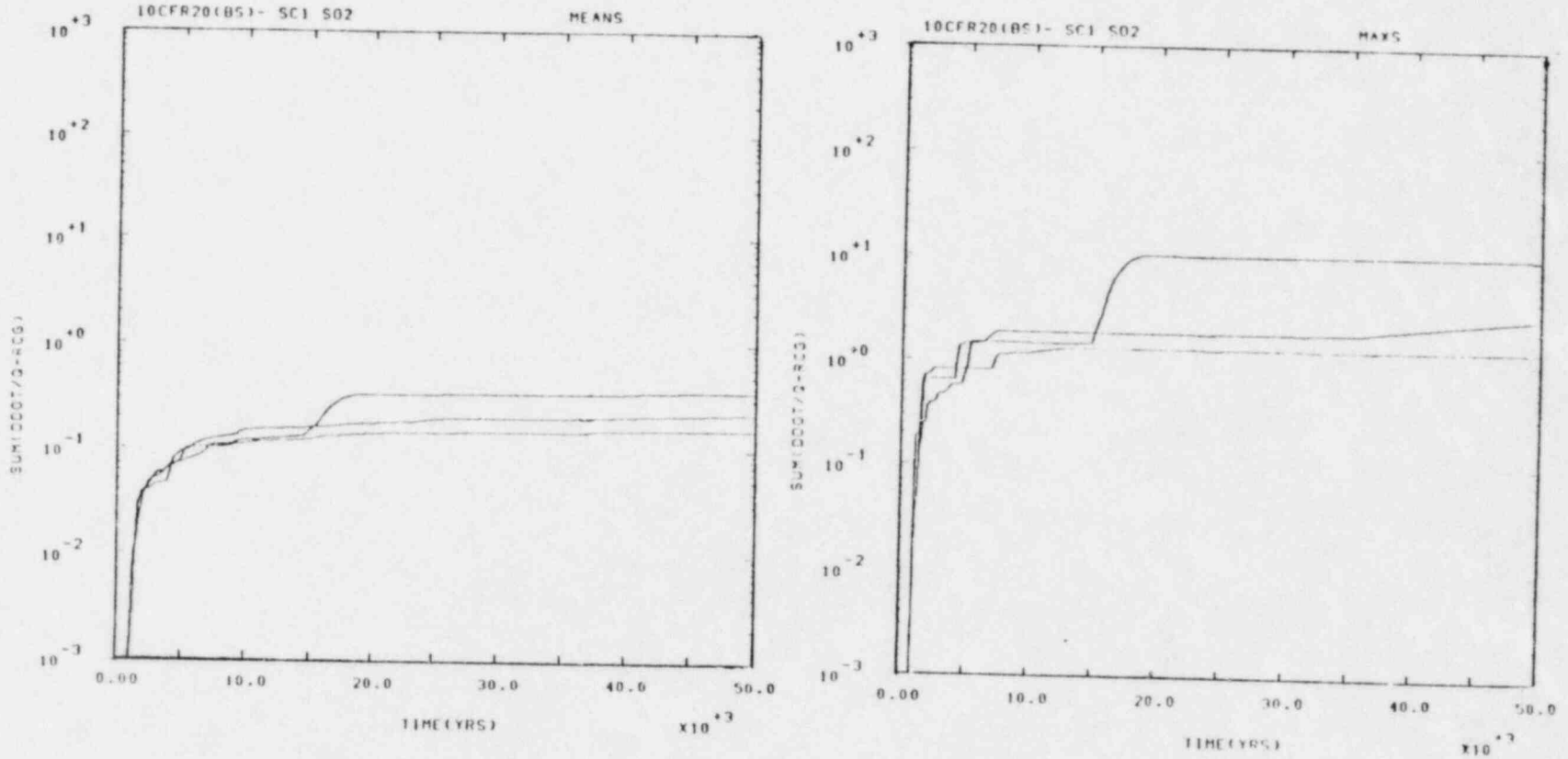

(a) (b)

Figure 18. Bedded Salt Scenario 1, Source 2, mean and maxiumum versus time

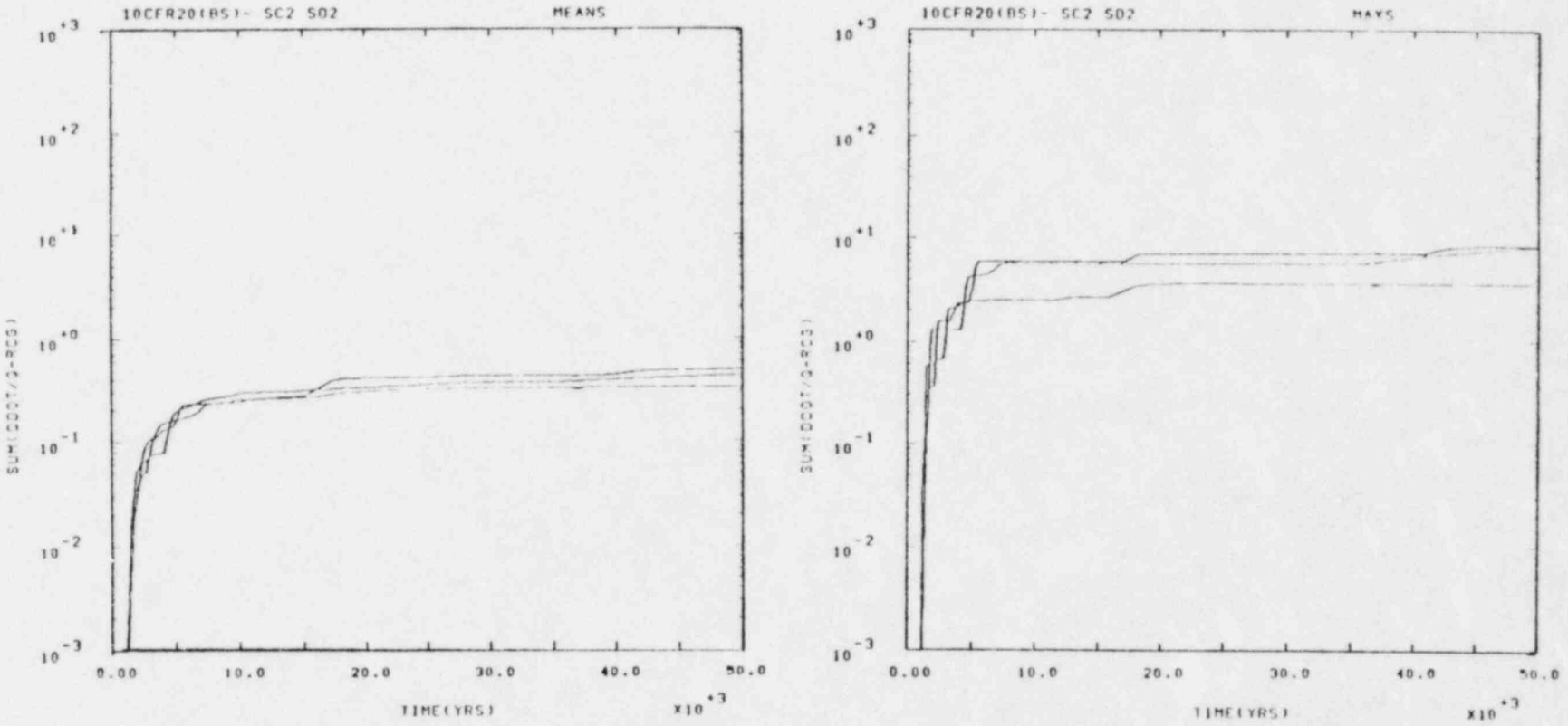

Figure 19. Bedded Salt Scenario 2, Source 2, mean and maximum versus time

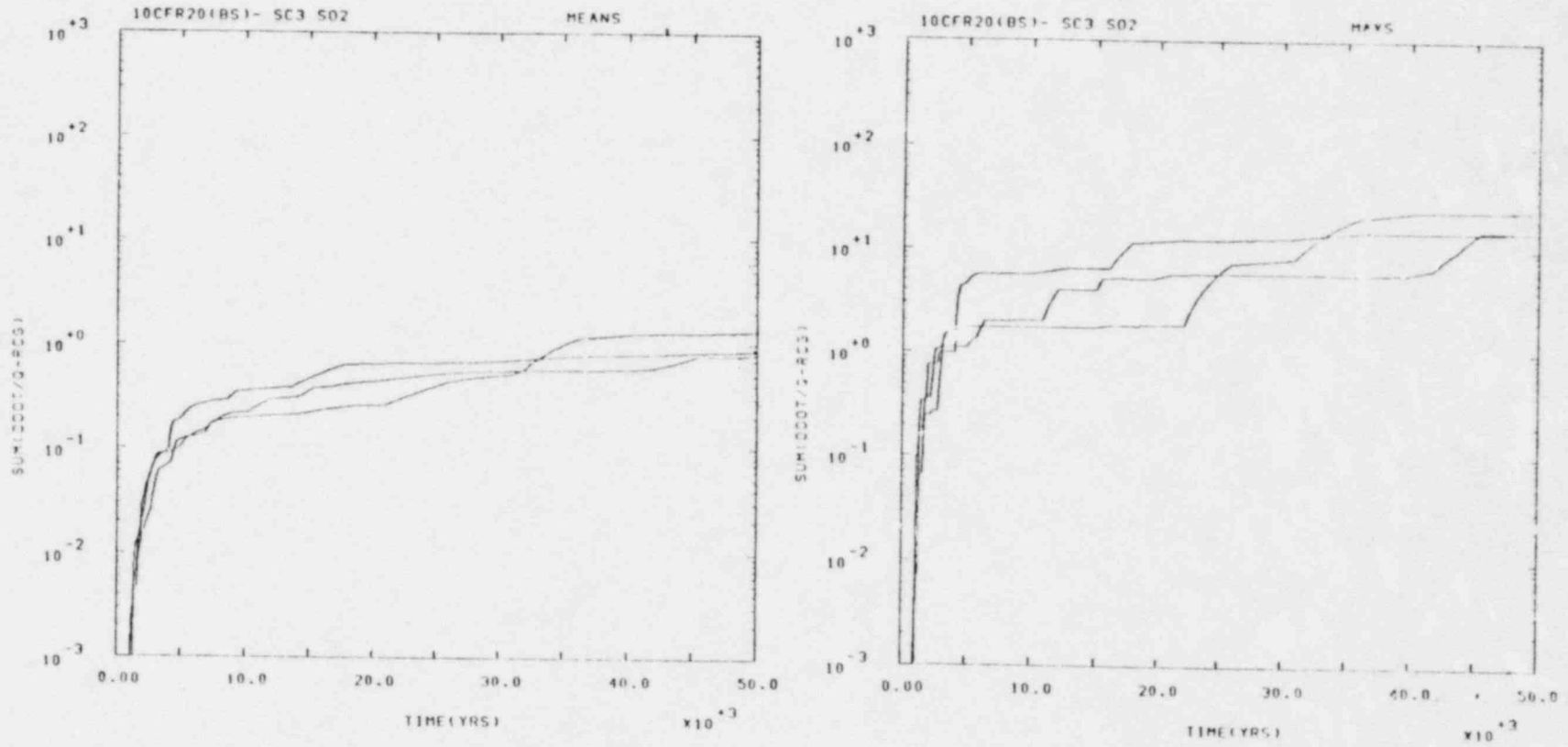

(a) (b)

Figure 20. Bedded Salt Scenario 3, Source 2, mean and maximum versus time

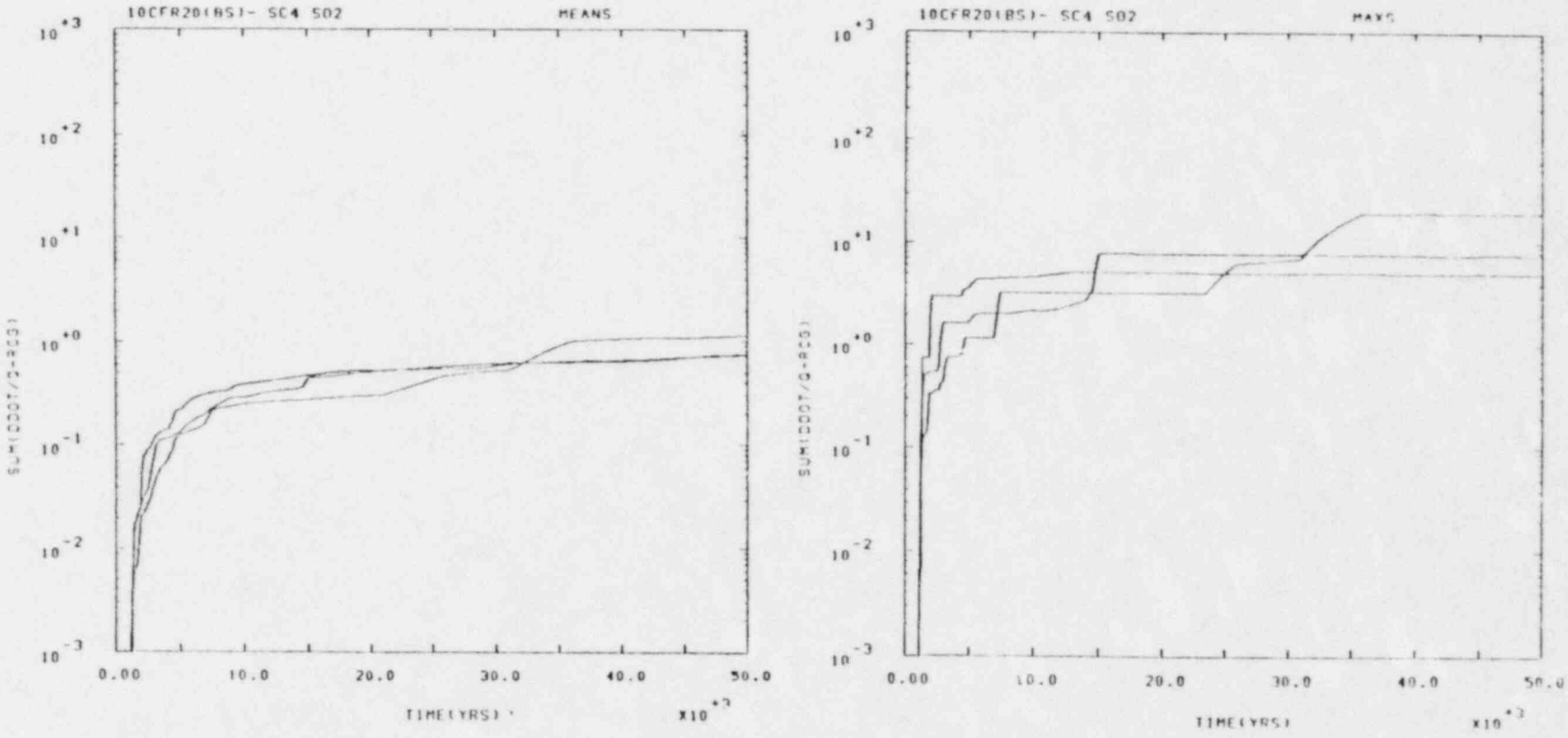

(a) (b)

Figure 21. Bedded Salt Scenario 4, Source 2, mean and maximum versus time

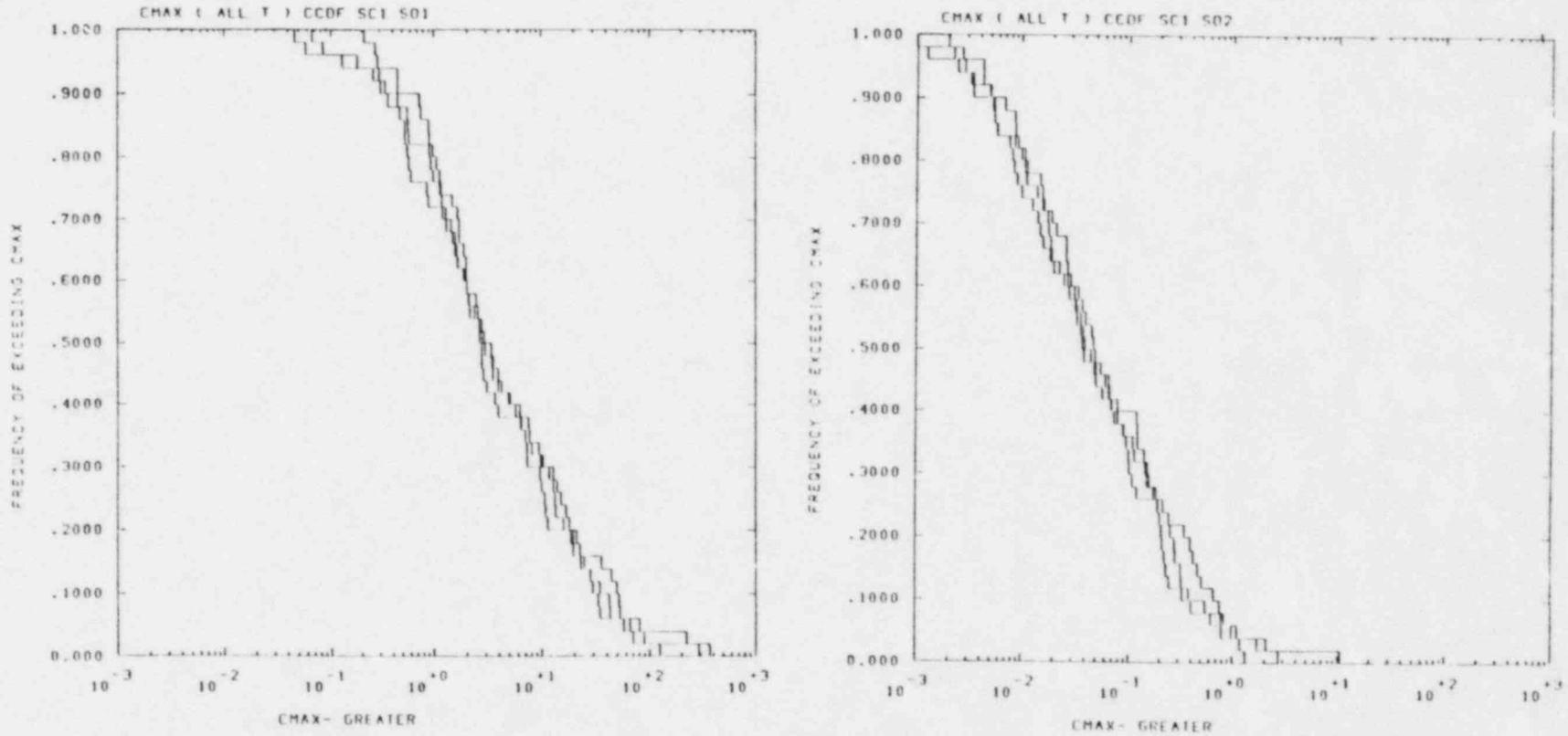

Figure 22. CCDF for Bedded Salt Scenario 1, Sources 1 and 2, maximum concentrations

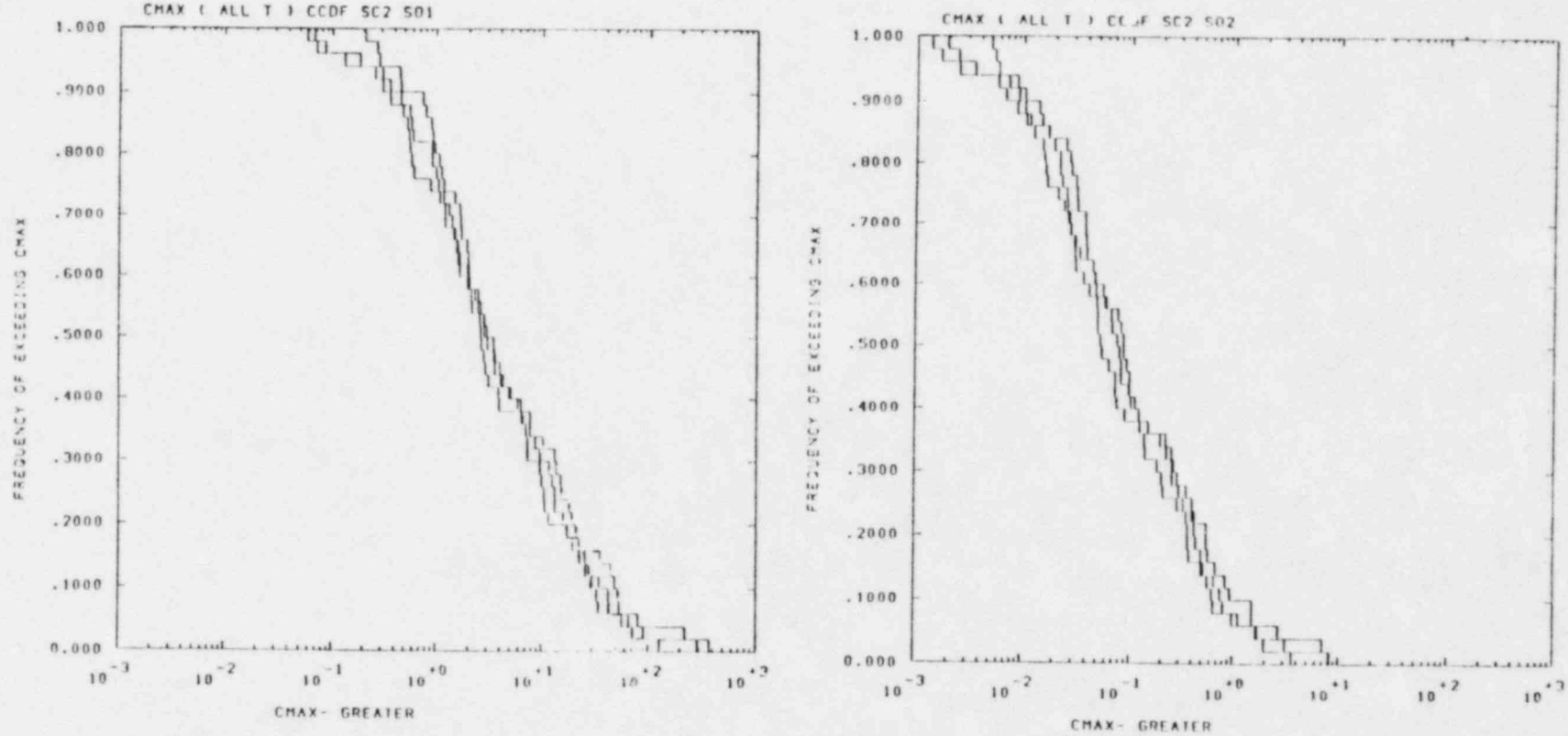

Figure 23. CCDF for Bedded Salt Scenario 2, Sources 1 and 2, maximum concentrations

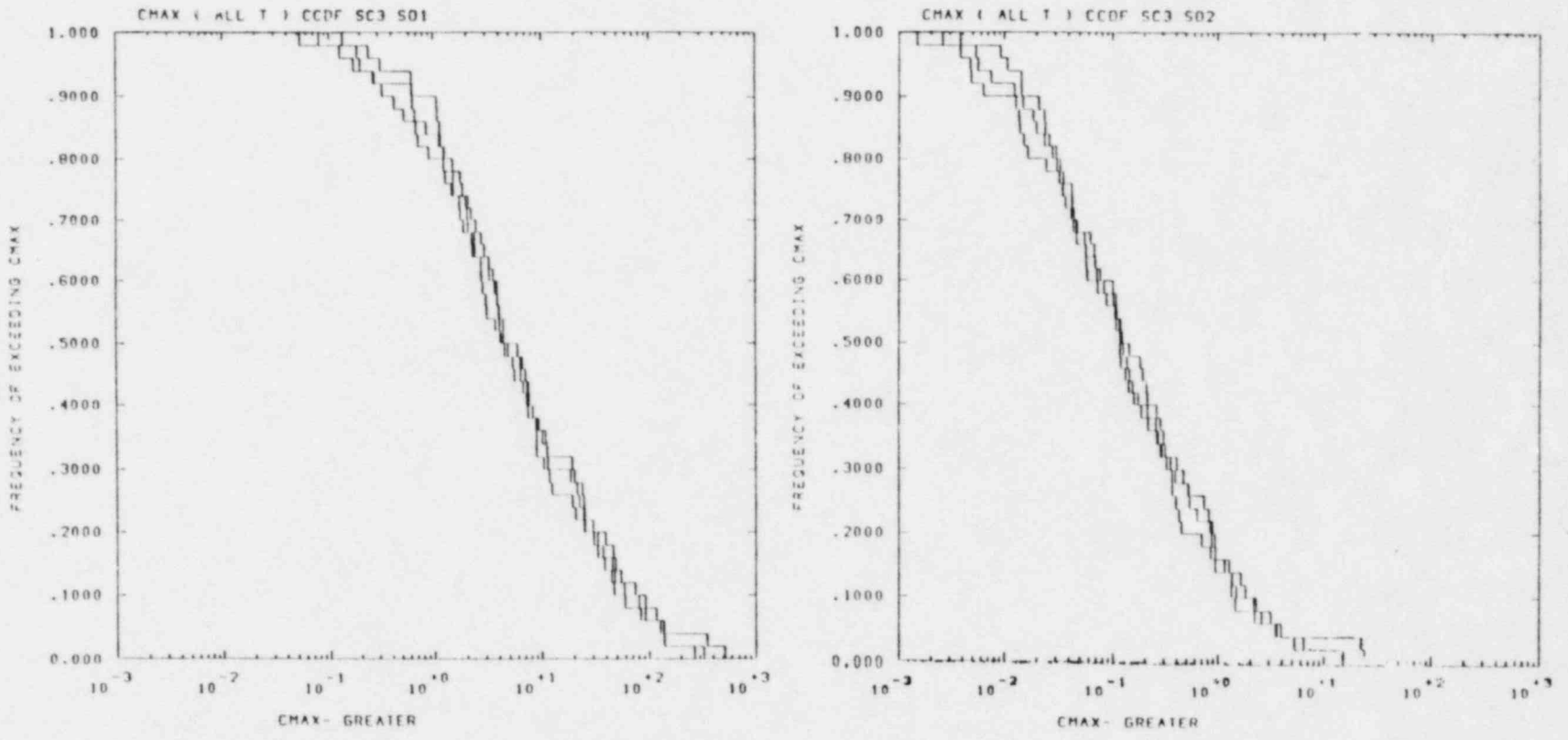

Figure 24. CCDF for Bedded Salt Scenario 3, Sources 1 and 2, maximum concentrations

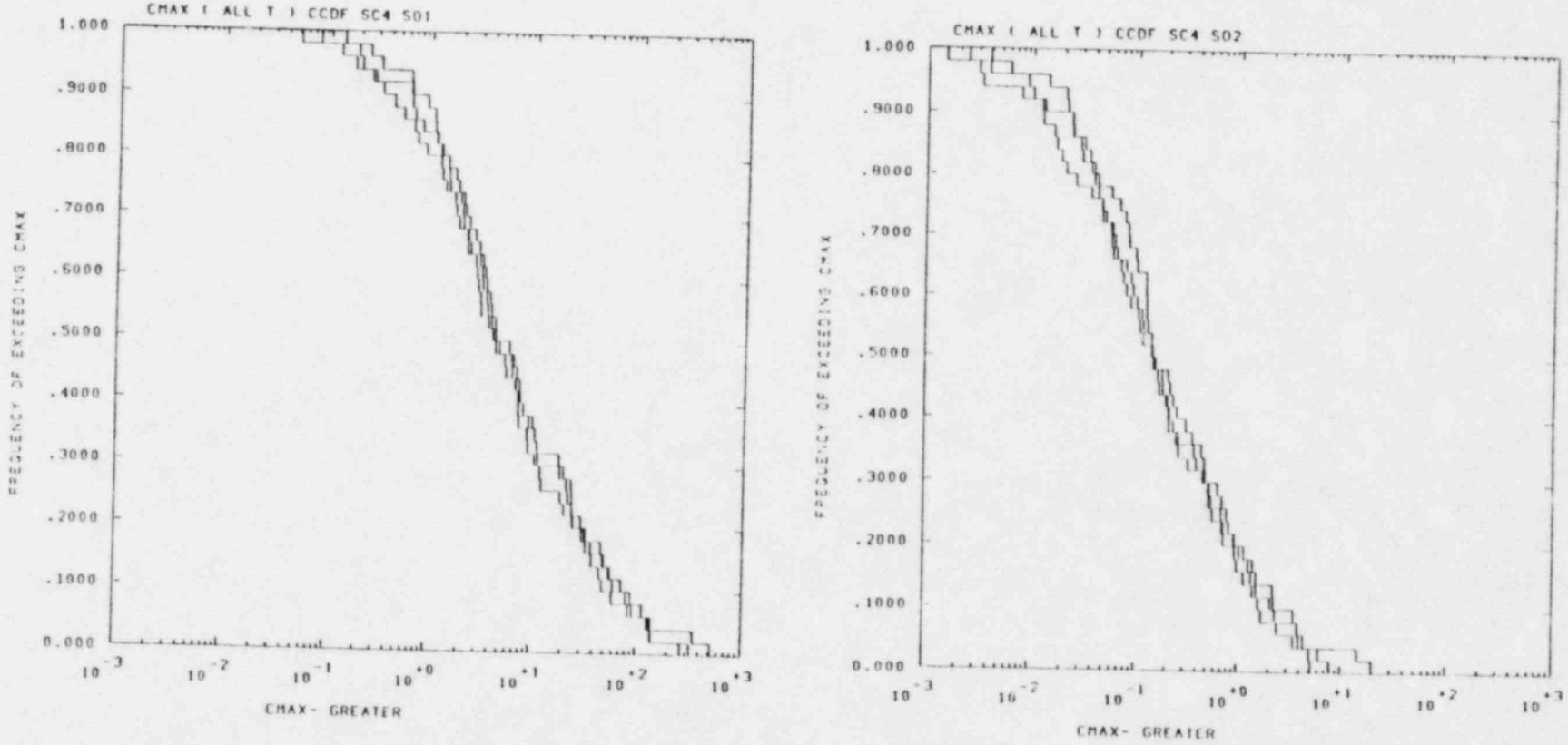

Figure 25. CCDF for Bedded Salt Scenario 4, Sources 1 and 2, maximum concentrations

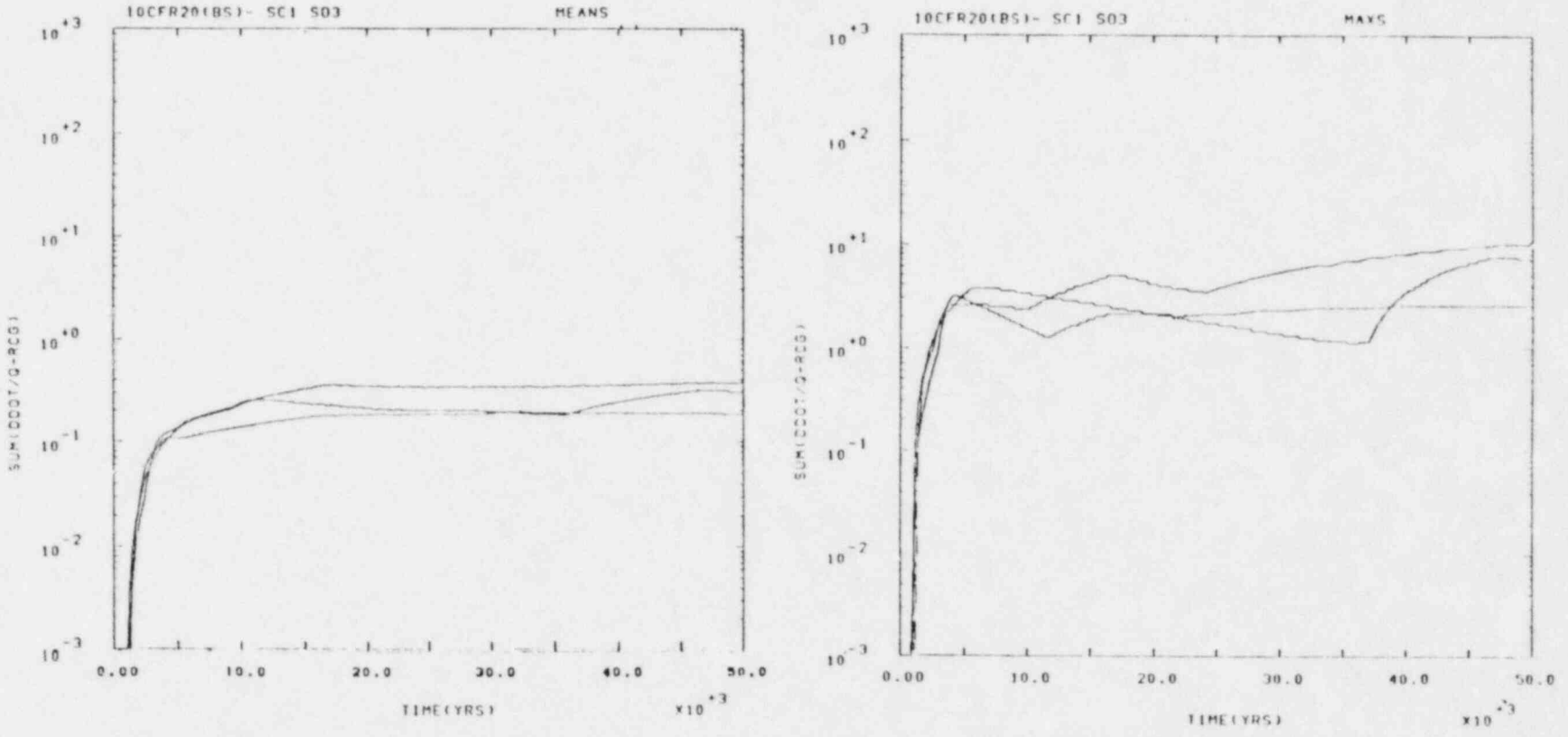

Figure 26. Bedded Salt Scenario 1, Source 3, mean and maximum versus time

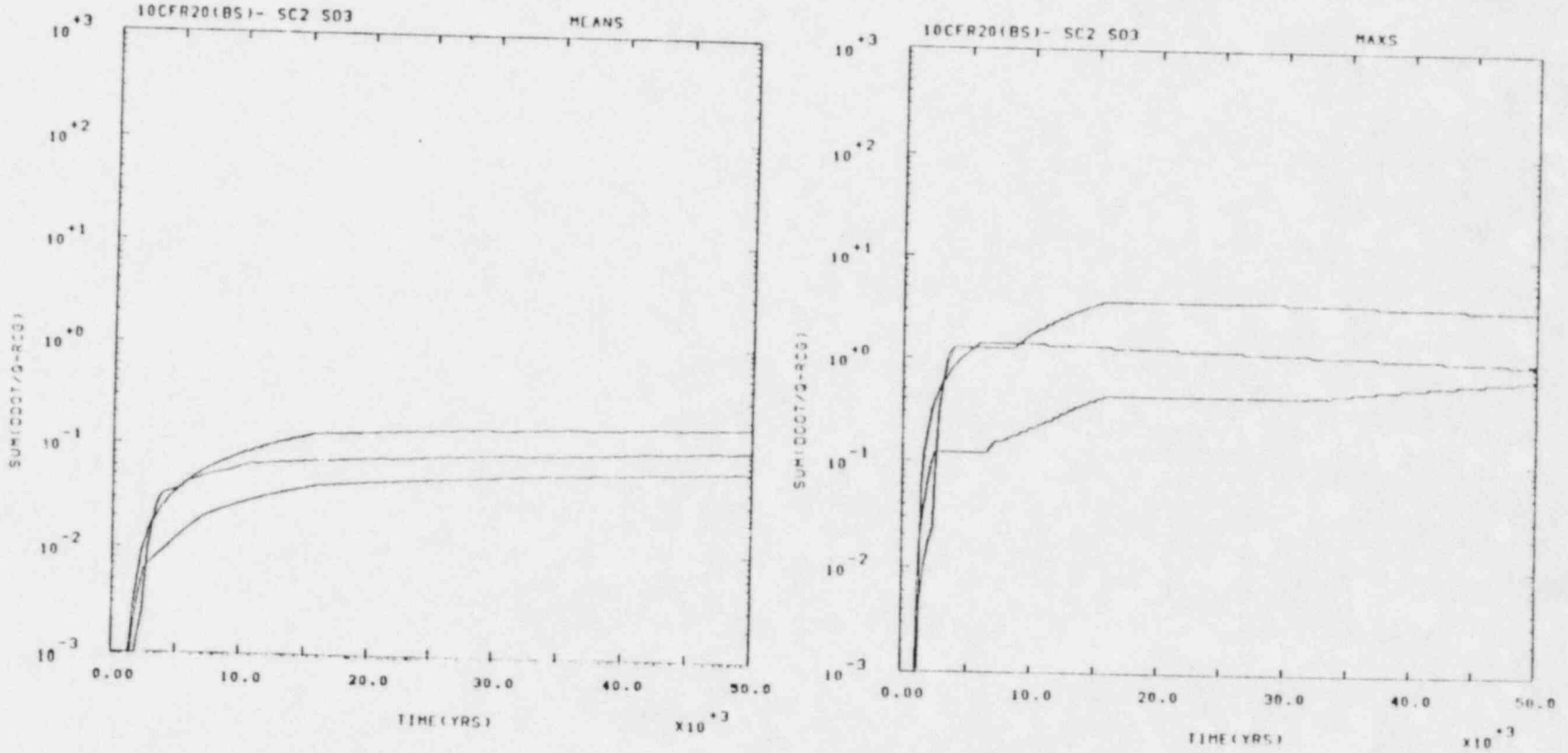

(a) (b)

Figure 27. Bedded Salt Scenario 2, Source 3, mean and maximum versus time

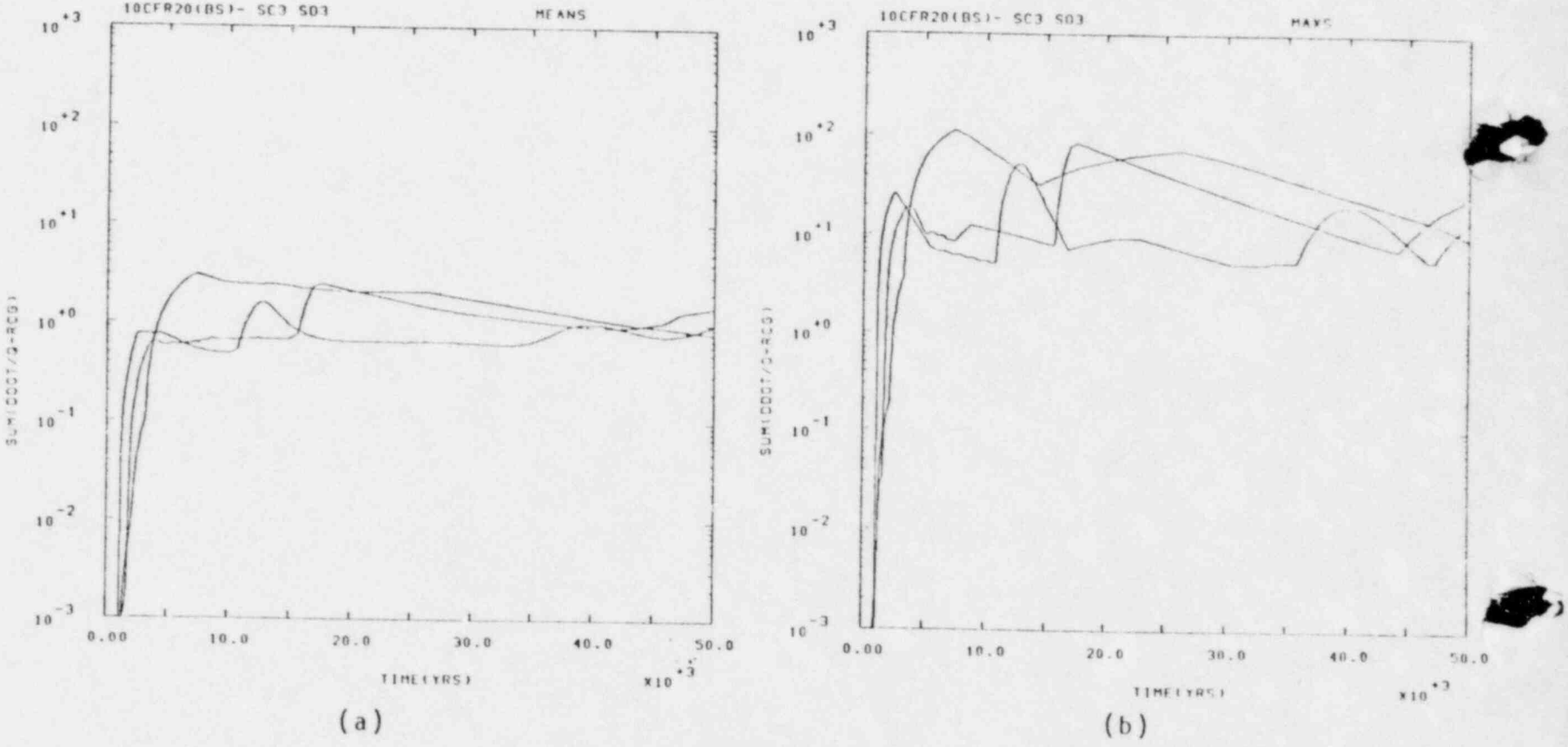

Figure 28. Bedded Salt Scenario 3, Source 3, mean and maximum versus time

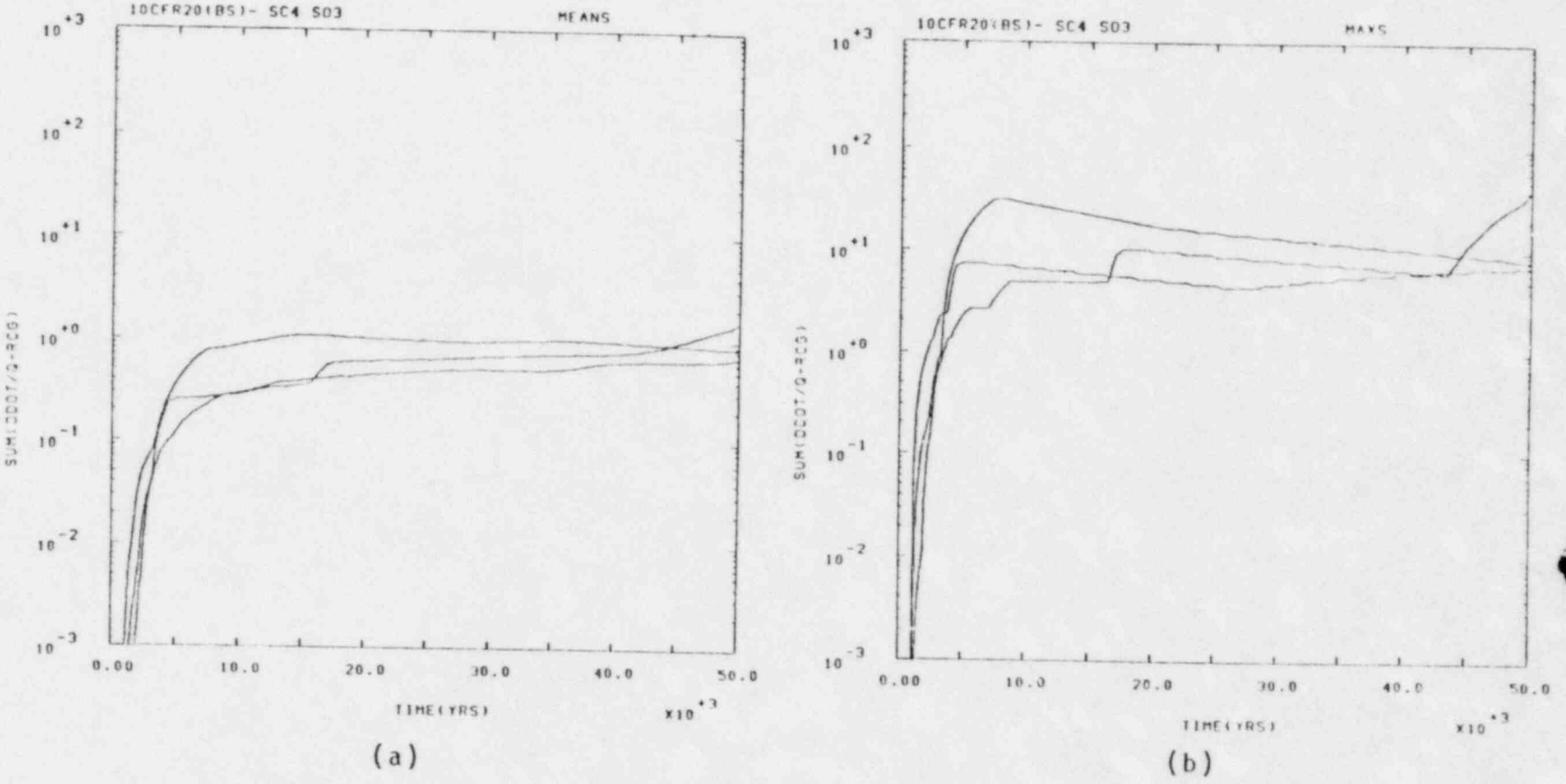

Figure 29. Bedded Salt Scenario 4, Source 3, mean and maximum versus time

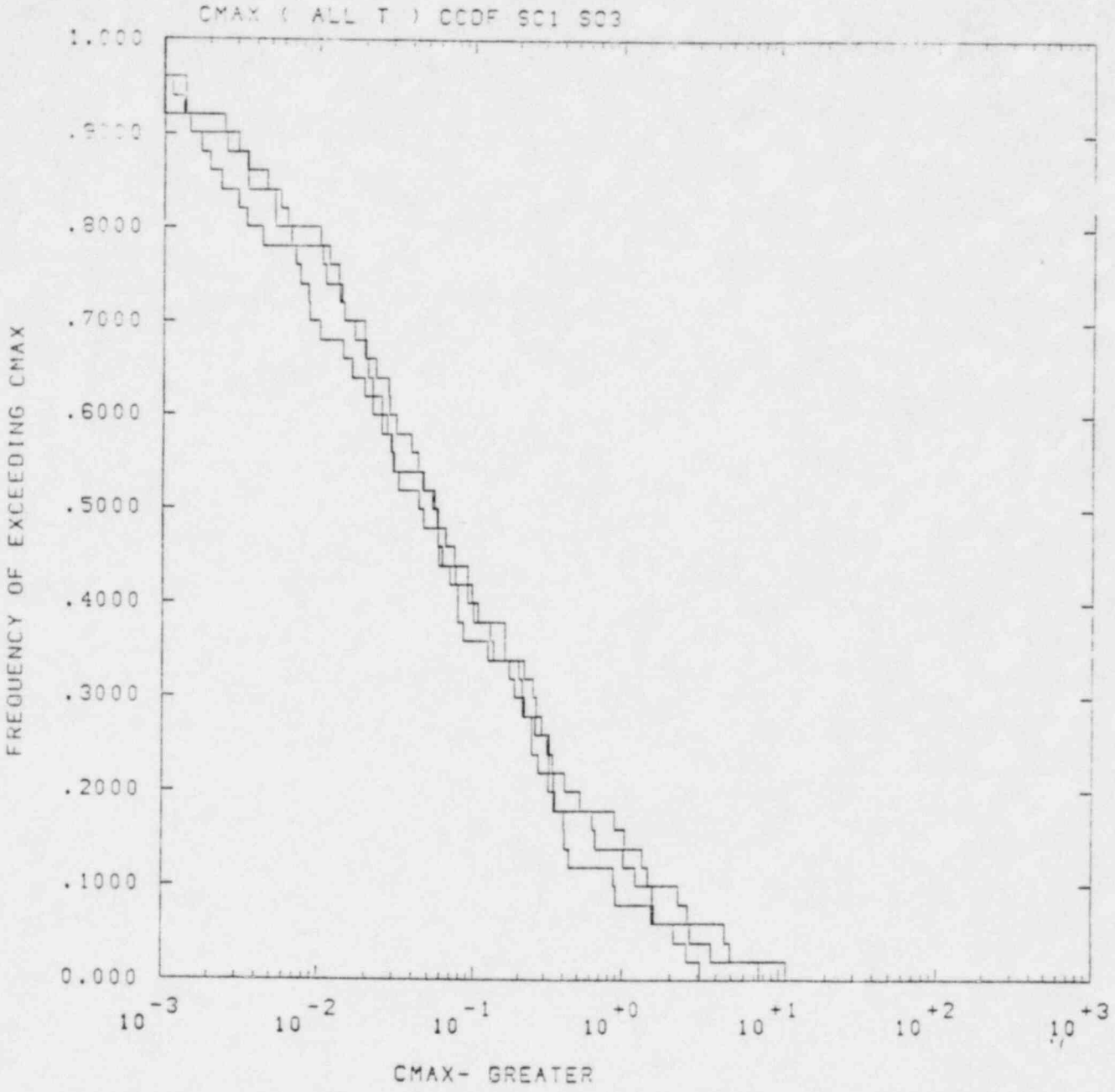

Figure 30. CCDF for Bedded Salt Scenario 1, Mixing Cell, maximum concentrations

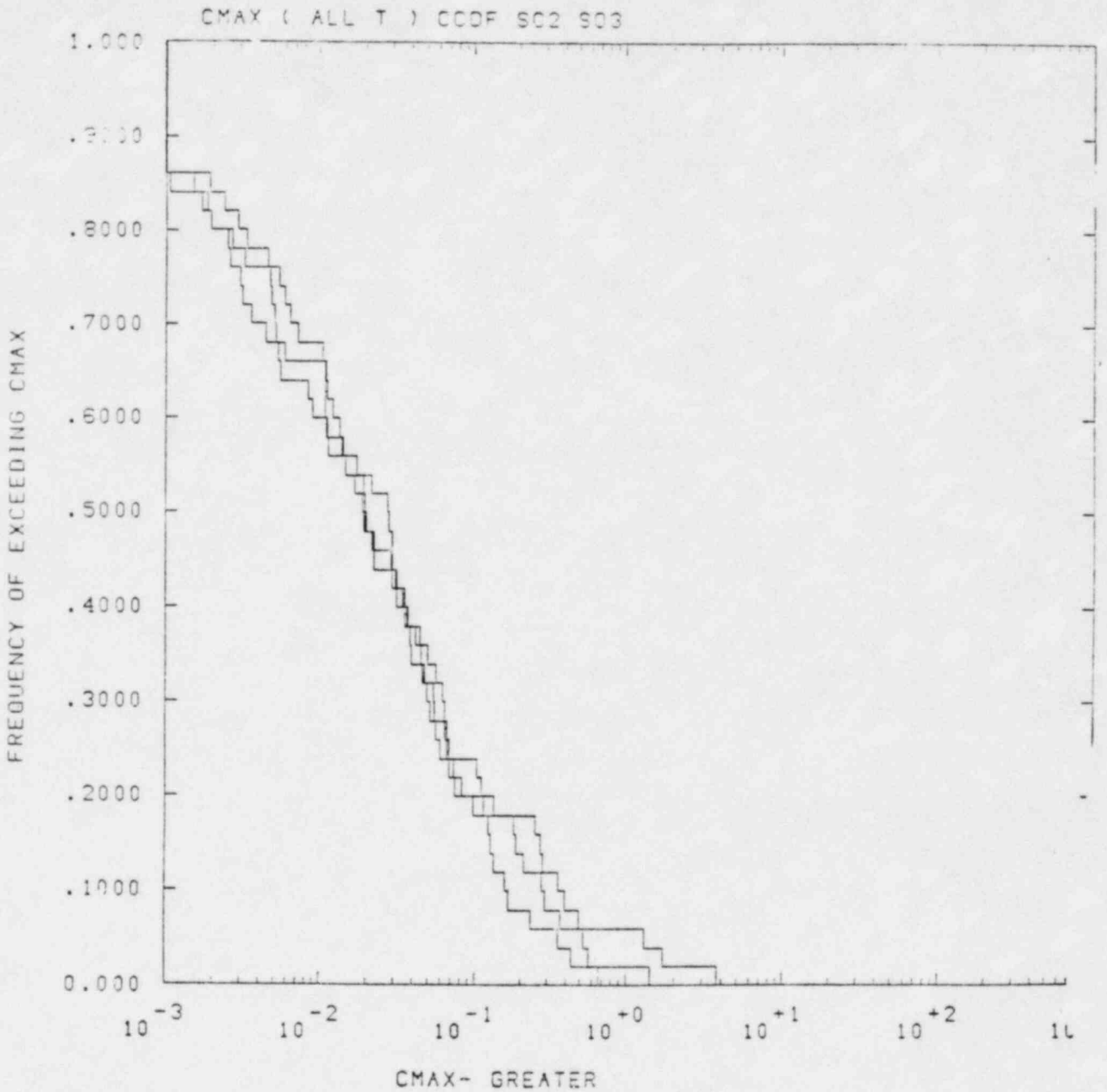

Figure 31. CCDF for Bedded Salt Scenario 2, Mixing Cell, maximum concentrations

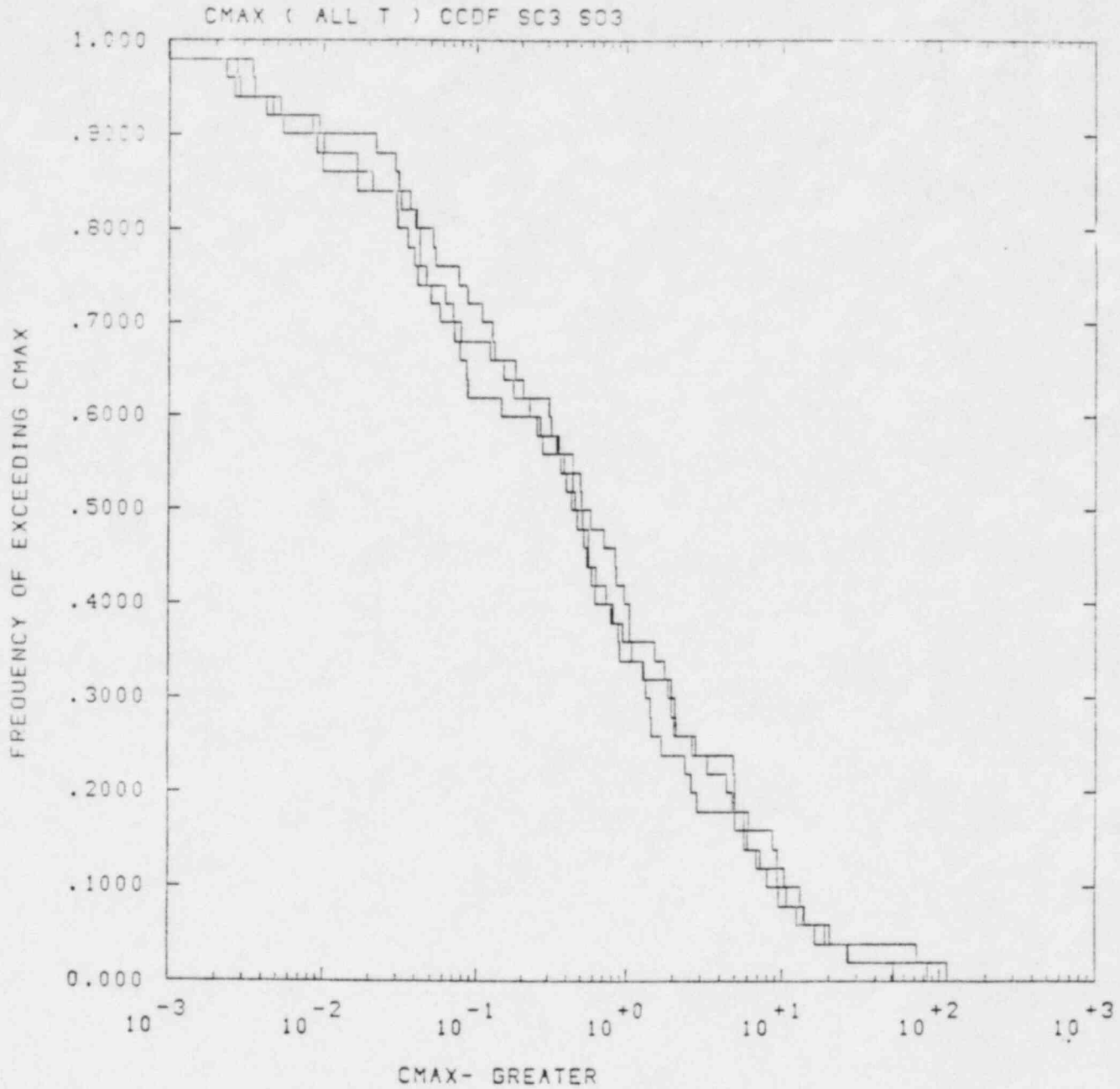

Figure 32. CCDF for Bedded Salt Scenario 3, Mixing Cell, maximum concentrations.

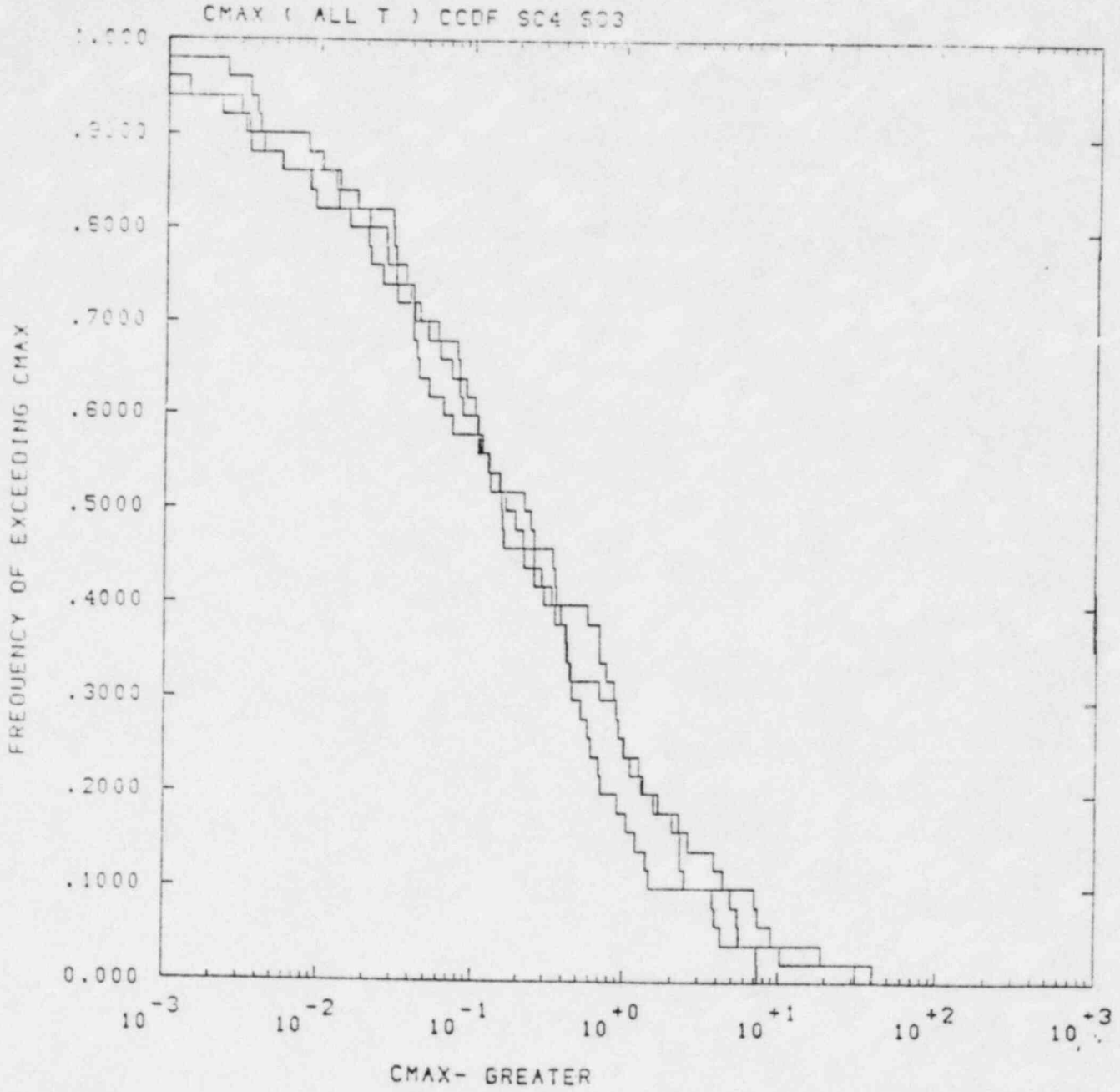

Figure 33. CCDF for Bedded Salt Scenario 4, Mixing Cell, maximum concentrations

Table 4

Important Radionuclides in Bedded Salt.
Scenarios (Based on First 50 Vectors)

Scenario:	1		2		3		4	
Source:	1 or 2	3	1 or 2	3	1 or 2	3	1 or 2	3
Radionulcide								
240Pu	6		6					
241Am								
237Np	38	6	39	6	13	1	11	1
233U			3	1	2	1		
238U	6	8	1	4	3	4	3	4
234U	24	21	21	18	25	17	24	20
226Ra	11	10	12	10	4	1	3	1
210Pb	2	4	2	2				
243Am	1	4	1	3				
239Pu	8	1	8	1				
235U						2		
231Pa	2	25	2	27	2	17	2	16
126Sn	43	20	43	21	38	24	38	24
135Cs	4	20	5	19	5	15	5	15
129I	50	50	50	30	43	44	43	44
99Tc	45	49	42	49	45	48	45	48
14C	31		43		47		47	

V. Conclusions

Using calculated results from a simple groundwater transport model, NWFT/DVM, and a simple Gaussian plume model to describe dispersion of radionuclides, we have estimated radionuclide concentrations in potential transporting aquifers and compared them to the standard for drinking water, 10CFR20. For many scenarios and source models analyzed, the probability of exceeding the 10CFR20 is non-zero. The value of the probability is given in Table 5. In particular, concentrations are high for many scenarios with a source model conceptually similar to but exceeding the minimum performance standards expressed in the draft 10CFR60 [8].

In performing these calculations a number of assumptions have been made which should be considered along with the results.

1. The calculated plume width is of a spatial extent comparable to that of the vertical extent of the aquifer. This may limit the vertical dispersion and dilution. However, we expect this effect to be relatively small and easily estimated.
2. The effects of large dilution volumes, as may be expected from a field of withdrawal wells rather than a single well, have been neglected.

Table 5

Probabilities of Exceeding
10CFR20 Requirements

Basalt

Scenario	1	2	3	4
	0	.3	.03	0

Bedded Salt

Scenario	1	2	3	4
Source				
1	.75	.75	.85	.85
2	.05	.10	.15	.15
3	.10	.05	.35	.20

Calculated results would be proportionately lower if dilution water was included.

3. Simple source terms have been assumed to describe the radionuclide release to the transporting aquifer. No detailed modelling of the source term has been performed. A potentially large reduction in concentrations may be achieved if the mixing cell assumption (Source #3) can be validated.

Further work in the description of radionuclide concentrations should address these areas.

VI. References

1. Pepping, R. E., Chu, M. S., and Siegel, M. D., "Technical Assistance for Regulatory Development - A Simplified Repository Analysis in a Reference Basalt Site," Sandia National Laboratories Report SAND82-0689, February 1982.

2. Pepping, R. E., Chu, M. S., and Siegel, M. D., "Technical Assistance for Regulatory Development : A Simplified Repository Analysis in a Hypothetical Bedded Salt Formation," Sandia National Laboratories Report SAND82-0996 (1982).

3. Campbell, J. E., Longsine, D. E., and Cranwell, R. M., "Risk Methodology for Geologic Disposal of Radioactive Waste - The NWFT/DVM Computer Code User's Manual," Sandia National Laboratories Report SAND81-0886, NUREG/CR-2081, November 1981.

4. U. S. Environmental Protection Agency, "Environmental Standards and Federal Radiation Protection Guidance for Management and Disposal of Spent Nuclear Fuel, High-Level and Transuranic Radioactive Wastes," 40CFR191, Draft 20, 1981.

5. Appendix B, Code of Federal Regulations, Title 10, Part 20.

6. Iman, R. L., Davenport, J. M., and Ziegler, D. K., Latin Hypercube Sampling (Program User's Guide), Sandia National Laboratories, SAND79-1473, January 1980.

7. Bennett, D. E., Sandia-ORIGEN User's Manual, NUREG/CR-0987, Sandia Laboratories, Albuquerque, NM, October 1979.

8. Nuclear Regulatory Commission, "Disposal of High Level Water in Geologic Repositories," 10CFR60, Federal Register, 48, July 8, 1981.